DM

Cell-Responsive Nanogels for Anticancer Drug Delivery

MASTER DISSERTATION

Dina Maria Sousa Maciel
MASTER IN APPLIED BIOCHEMISTRY

UNIVERSIDADE da MADEIRA
A Nossa Universidade
www.uma.pt

September | 2014

Cell-Responsive Nanogels for Anticancer Drug Delivery

MASTER DISSERTATION

Dina Maria Sousa Maciel
MASTER IN APPLIED BIOCHEMISTRY

SUPERVISOR
Yulin Li

CO-SUPERVISOR
Helena Maria Pires Gaspar Tomás

CELL-RESPONSIVE NANOGELS FOR ANTICANCER DRUG DELIVERY

Tese apresentada à Universidade da Madeira com vista à obtenção do grau de Mestre em Bioquímica Aplicada

Dina Maria Sousa Maciel

Sob a orientação de:

Doutor Yulin Li

Professora Doutora Helena Maria Pires Gaspar Tomás

Centro de Competências de Ciências Exatas e da Engenharia,

Centro de Química da Madeira

Funchal – Portugal

Setembro 2014

Acknowledgments

The accomplishment of this master thesis was possible due to several people and I am grateful to everyone that helped and contributed in any way to the execution of my project.

I want to acknowledge my supervisor Dr. Yulin Li for the support and for all the help in clarifying and understanding during this project work.

To my supervisor Prof. Dr. Helena Tomás, for all the goodwill and motivation throughout the year. And to whom I also show my appreciation for the readiness and generosity.

To Prof. Dr. João Rodrigues and CQM for the support and for providing the facilities to carry out this project.

I also would like to acknowledge Prof. Xiangyang Shi (CQM/UMa, Portugal and Donghua University, Shanghai) for his collaboration, especially for the Scanning Electron Microscopy analyses.

I am also grateful for the help and the readiness of the laboratory technicians Paula Andrade and Paula Vieira, for providing the lab materials and reagents and in all that I needed.

To my colleagues of the Molecular Materials Research Group (MMRG) for all the support and enthusiasm. In particular, to my friends and colleagues Mara Gonçalves, Carla Alves, Débora Capelo, Rita Castro, Cláudia Camacho, Nilsa Oliveira and Manuel Jardim for their friendship, support and motivation. A special thanks to Mara, Rita, Débora and Carla for the precious help in this project work.

To my dearest friends and Master colleagues Marisa Faria, Igor Fernandes, João Micael Leça, and Marisela Santos for their friendship, support, enthusiasm and motivation during this year, and for being always available.

I want to demonstrate my true and special thanks to my parents for their endless support, concern and love. A special thanks to my brother Francisco, for always supporting and encouraging me all the time.

This master project was financially supported by Fundação para a Ciência e a Tecnologia (FCT) through the Projects PTDC/CTM-NAN/112428/2009 and PTDC/CTM-NAN/116788/2010, the NMR Portuguese Network (PTNMR-2014) and the CQM strategic project (Ref. PEst-OE/QUI/UI0674/2014). The work of Dr. Yulin Li (my supervisor) at CQM was possible through the FCT Science 2008 Programme. For these reasons, I am deeply grateful to FCT.

A great and sincere THANK YOU to all whom, directly or indirectly, contributed in my training.

This Master thesis was performed at Centro de Química da Madeira (CQM), University of Madeira, consisting in the preparation and characterization of nanogels for drug delivery.

For the student, it was an opportunity to learn/gain more experience on techniques used in the preparation of nanogels, more specifically in emulsion methods, as well as in bioconjugation synthetical procedures. The student also worked on animal cell culture, UV-Vis, Fourier transformed infrared and fluorescence spectroscopies, dynamic light scattering and zeta potential measurements, and fluorescence microscopy.

Abstract

One of the main goals in Nanomedicine is to create innovative drug delivery systems (DDS) capable of delivering drugs into a specific location with high efficiency. In the development of DDS, some essential properties are desired, such as biocompatibility and biodegradability. Furthermore, an ideal DDS should be able to deliver a drug in a controlled manner and minimize its side effects. These two objectives are still a challenge for researchers all around the world.

Nanogels are an excellent vehicle to use in drug delivery and several other applications due to their biocompatibility. They are polymer-based networks, chemically or physically crosslinked, with at least 80-90% water in their composition. Their properties can be tuned, like the nanogel size, multifunctionality and degradability. Nanogels are capable of carrying in their interior bioactive molecules and deliver them into cells.

The main objective of this project was to produce nanogels for the delivery of anticancer drugs with the ability of responding to existent stimuli inside cells (cell-responsiveness nanogels) and/or of controlled drug delivery. The nanogels were mainly based on alginate (AG), a natural biopolymer, and prepared using emulsion approaches. After their synthesis, they were used to encapsulate doxorubicin (Dox) which was chosen as a model drug. In the first part of the experimental work, disulfide-linked AG nanogels were prepared and, as expected, were redox-sensitive to a reducing environment like the intracellular medium. In the second part, AG nanogels crosslinked with both calcium ions and cationic poly(amidoamine) dendrimers were developed with improved sustained drug delivery. The prepared nanogels were characterized in terms of size, chemical composition, morphology, and drug delivery behavior (under redox/pH stimuli). The *in vitro* cytotoxicity of the nanogels was also tested against CAL-72 cells (an osteosarcoma cell line).

Keywords: drug delivery, nanogels, cell-responsiveness, alginate, anticancer

Resumo

Um dos principais objetivos da Nanomedicina é criar um sistema inovador de entrega de fármacos, capaz de entregar com elevada eficácia os fármacos em locais específicos. No desenvolvimento destes, são desejáveis propriedades como a biocompatibilidade e a biodegradabilidade. Um sistema de entrega de fármacos ideal é capaz de entregar o fármaco e minimizar os efeitos secundários a ele associados. Estes dois objetivos continuam a representar um desafio para os investigadores de todo o mundo.

Os nanogéis são constituídos por redes à base de polímeros reticulados química ou fisicamente, com pelo menos 80-90% de água na sua composição. São um excelente veículo para uso na entrega de fármacos e em várias outras aplicações por apresentarem excelente biocompatibilidade. Devido à sua estrutura, os nanogéis podem transportar no seu interior moléculas ativas e entregá-las nas células. As suas propriedades podem ser controladas, tais como o tamanho, a multifuncionalidade e a degradabilidade.

O principal objetivo deste projeto foi criar nanogéis para a entrega de fármacos anticancerígenos com a capacidade de responder a estímulos presentes no interior das células e/ou de libertar o fármaco de forma controlada. Os nanogéis foram constituídos à base de alginato (AG), um biopolímero natural, e sintetizados utilizando métodos de emulsão. Após a sua síntese, os nanogéis foram usados no encapsulamento de doxorrubicina (Dox), escolhida como fármaco modelo. Na primeira parte do trabalho experimental, foram preparados nanogéis de AG reticulados através de pontes dissulfureto e capazes de responder a ambientes redutores como aqueles existentes no interior das células. Na segunda parte, desenvolveram-se nanogéis de AG reticulados por ligações estabelecidas por iões cálcio e dendrímeros catiónicos de poli(amidoamina) com uma capacidade melhorada de entregar o fármaco de forma controlada. Estes nanogéis foram caracterizados em termos de dimensão, composição química, morfologia e comportamento de libertação do fármaco (sob estímulos do tipo redox/pH). A citotoxicidade dos nanogéis foi também testada usando células CAL-72 (uma linha de células de osteossarcoma).

Palavras-chave: entrega de fármacos, nanogéis, responsividade celular, alginato, anticancerígeno

Table of Contents

List of Figures

List of Tables

List of Acronyms

AA	Antibiotic-antimycotic
Abs	Absorbance
AG	Alginate
AOT	Dioctyl sodium sulfosuccinate
C_r	Cumulative release
CST	Critical solution temperature
Cys	Cystamine
DAPI	4',6-diamidino-2-phenyindole dilactate
DCM	Dichloromethane
DDS	Drug delivery system
DLS	Dynamic light scattering
D-MEM	Dulbecco's modified eagle medium
DMSO	Dimethyl sulfoxide
DNA	Deoxyribonucleic acid
Dox	Doxorubicin
DTT	D,L-dithiothreitol
EDC	1-ethyl-3-(3-dimethylamino propyl)carbodiiamide hydrochloride
EPR	Enhanced permeation and retention
FBS	Fetal bovine serum
FDA	Food and Drug Administration
FI	Fluorescein isothiocyanate
FTIR	Fourier transformed infrared spectroscopy
G5	Generation 5
GILT	γ-interferon-inducible lysosomal thiol reductase
GSH	Glutathione
hMSC	Human mesenchymal stem cells
IC_{50}	Half maximal inhibitory concentration
ITS	Insulin-transferrin-selenium
LCST	Lower critical solution temperature
MWCO	Molecular weight cut off
NMR	Nuclear magnetic resonance
PAMAM	Poly(amidoamine)

PBS	Phosphate buffer saline
PEG	Polyethylene glycol
PGA	Polyglycolic acid
pK_a	Acid dissociation constant
PLGA	Poly(lactic-co-glycolic acid)
PNIPAM	Poly(*N*-isopropylacrylamide)
PVA	Polyvinyl alcohol
RES	Reticuloendothelial system
RNA	Ribonucleic acid
rpm	Revolutions per minute
SEM	Scanning electron microscopy
UCST	Upper critical solution temperature
UP	Ultrapure
UV-Vis	Ultraviolet-visible spectroscopy

CHAPTER I. General Introduction

1. GENERAL INTRODUCTION

1.1. Drug Delivery Systems

Nowadays, nanoscience and nanotechnology are getting a huge attention due to the advances that they are bringing to different scientific areas. The biomedical field, for example, is one with increasing research developments and with real applications in diagnosis, prevention and treatment of several diseases[1, 2]. Other applications include tissue engineering, biomedical implants and bionanotechnology[3].

Nanomedicine strongly relies on drug delivery systems (DDS) at the nanoscale which shows unique physical, chemical and biological properties[1]. DDS are being developed to target and treat specific areas in the body taking advantage of complex formulations and drug delivery controlled release[4]. The DDS can also be designed having in mind the type of administration route which can be oral, intravenous, arterial, transdermal, suppository, nasal, subcutaneous, sublingual, amongst others[5]. Issues related to low aqueous solubility of some drugs, drug degradation by the biological system leading to lower drug efficiency and undesirable drug accumulation in organs or tissues are unwanted effects that nanoscience need to control[5]. In anticancer therapy, for example, the DDS are often administrated directly intravenously and it is important that the drug diffuses from the bloodstream to the exact location, more specific/precisely to the tumor cells[6].

To accomplish the nanomedicine objectives, one should consider some factors when designing DDS, like the chemical and physical properties of the drug, the route of administration, the nature of the delivery vehicle, the drug release mechanism, the potential for cell/tissue targeting and, above all, the biodegradability and biocompatibility of the system[4, 7, 8]. All these factors have a huge impact when designing an ideal DDS, but are not easy to be taken in mind in a single system.

The main goal to develop DDS is to improve the bioavailability and pharmacokinetics of the therapeutic agents, with systems capable of passing through the biological barriers and deliver the drugs into a specific location[1, 9, 10]. However, DDS still present some problems that need to be overcome, like poor intracellular delivery, lack of control over the release behavior and difficulty in targeting the diseased cells/tissues which can lead to important side effects (the DDS, themselves, can show some toxicity)[11]. In summary, DDS should: present a high loading capacity; maintain an optimal therapeutic drug concentration in the blood; show a sustained drug delivery with predictable and reproducible release rates with no early drug release; enhance the activity duration of short half-life drugs; target specific cells and

tissues; conduct to reduced side effects by being made of biocompatible/biodegradable materials; and allow patient compliance and optimized therapy[4, 5, 12]. One important fact is that these systems can even modulate and change the biodistribution profile of the drugs depending on the different methods of administration[1]. Furthermore, with the use of an ideal DDS, just a minor amount of drug will be required to obtain a therapeutic effect and a decrease on the side effects[13].

1.2. Drug delivery systems based on polymers

The DDS used in nanomedicine include viral vectors, polymer-based vehicles (*e.g.* dendrimers, peptides and polymersomes), lipid based nanosystems (*e.g.* micelles and liposomes), carbon nanotubes, and inorganic nanomaterials (*e.g.* nanodiamonds, gold and mesoporous silica nanoparticles) (Figure 1)[2, 14].

DDS based on polymer are from utmost importance. For their preparation, the polymers can be from natural or synthetic origin and degradable or nondegradable. Natural polymers are polysaccharides, such as alginate[15, 16], chitosan[7], gelatin[15], cellulose[7], hyaluronic acid[17], amongst others[18]. These natural polymers are abundant in nature, from renewable sources, with low cost, nontoxic, and present a high content of functional groups (such as hydroxyl, amino and carboxylic acid groups) that can be used in reactions for further bioconjugation (for example, with the purpose of cell targeting)[3, 18, 19]. Synthetic polymers are those that are produced by polymerization, such as dendrimers[9], polyglycolic acid (PGA)[7], polyethylene glycol (PEG)[9, 13, 17], and poly(lactic-co-glycolic acid) (PLGA)[7, 20]. Compared to natural polymers, synthetic ones have better controllable physicochemical properties. Degradable polymers contain labile bonds such as ester-, amide- and anhydride-bonds that are susceptible to hydrolysis or enzymatic degradation (surface degradation or bulk degradations)[21]. These DDS based on polymers can physically encapsulate bioactive molecules within the polymeric network, including small drugs, proteins, and DNA/RNA. Alternatively, they can immobilize the bioactive molecules through chemical linkages. The incorporation of inorganic materials (such as quantum dots, and magnetic and gold nanoparticles) inside the polymer structure can also be done to obtain multifunctional systems (theranostic systems) that may have a therapeutic action beyond drug delivery[22].

Actually, these polymer-based DDS can be found in a vast diversity of designs/architectures such as linear or branched polymers, dendrimers, polymersomes, and micelles, alone or in combination with other chemical entities/nanomaterials[9].

The design of a polymer-based nanocarrier is important for its chemical, interfacial, mechanical and biological functions[4]. For example, the nanocarrier surface properties, such as hydrophilicity, lubricity, smoothness and surface energy, have a strong influence on its interaction with tissues and blood. Other important properties of a nanocarrier is its durability, permeability and degradability[4].

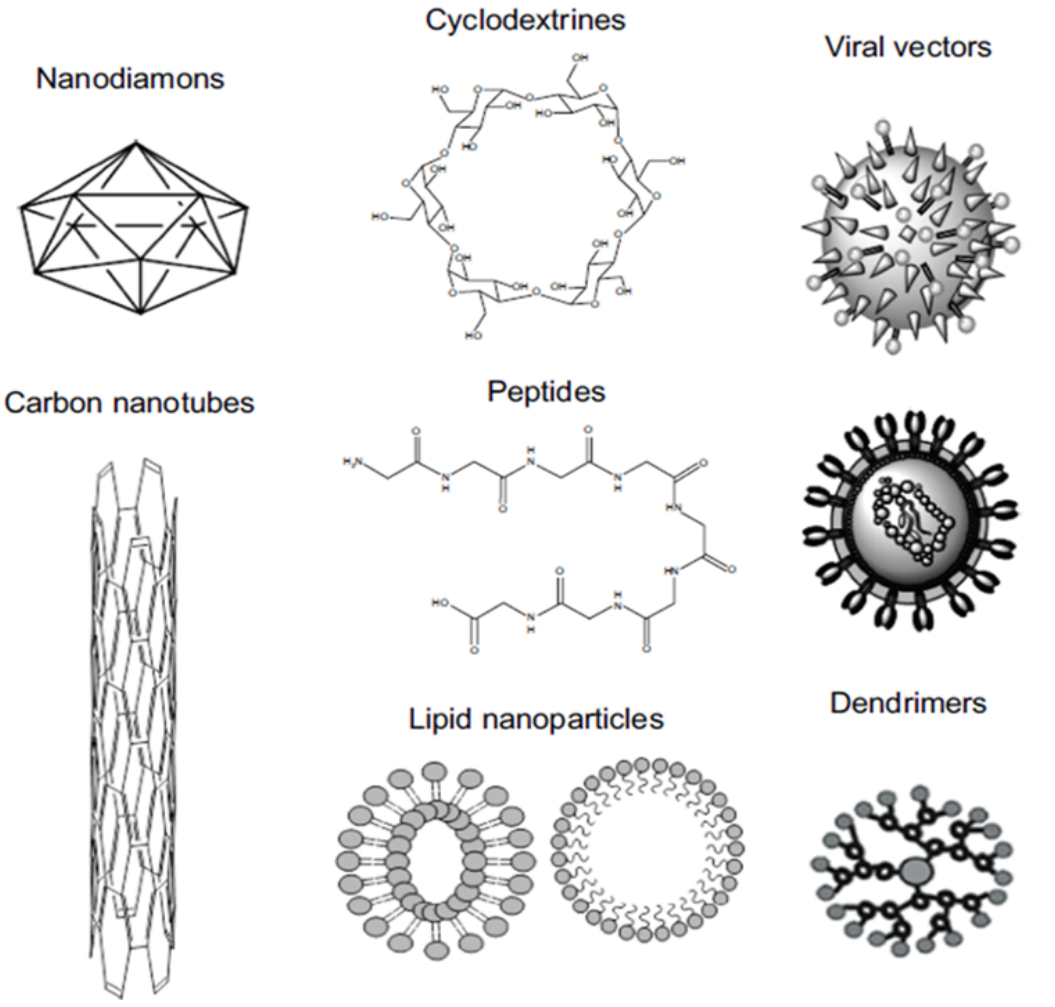

Figure 1. Types of nanocarriers used for transporting drugs, nucleic acids or proteins (adapted from reference 2).

1.3. Nanogels

Nanogels are a special group of DDS based on hydrophilic polymers (it retains water in their structure). They are crosslinked hydrogel particles[3], within a size range between 10^{-9} m (nanometer) and 10^{-6} m (micrometer)[9, 19]. Nanogels are an important class of

nanomaterials that have excellent interior structures for drug encapsulation[7], and present all the properties of the bulk hydrogels, but at the nanoscale dimensions. So, nanogels are crosslinked polymeric particles with a high water content.

The crosslinking in nanogels can be established by non-covalent physical associations, covalent chemical linkages, or combinations between them[23]. The crosslinking methods that can be used to prepare nanogels include the use of ions, radiation, molecules with special functional groups, self-assembly, crystallization and crosslinking polymerization[24]. Nanogels formed by physical crosslinking occur *via* non-covalent attractive forces, namely hydrophilic-hydrophilic interactions, hydrophobic-hydrophobic interactions, ionic interactions and/or hydrogen bonding[23, 24]. The properties of these nanogels are dependent on polymer/crosslinking agent composition and concentration, temperature and ionic strength of the medium. Nanogels formed by chemical crosslinking imply the reaction between crosslinking points along the backbone of the polymer chain[24] and usually makes use of crosslinking molecules. The properties of these nanogels (such as porosity and swelling) are strongly determined by the type of crosslinker and the extent of crosslinking reactions. The chemically crosslinked nanogels are, in principle, more stable than the physically crosslinked[23] but the use of crosslinkers may raise concerns related with toxicity[13].

Because water is in their composition in large percentage, nanogels are usually biocompatible, and have suitable mechanical properties for DDS formulation[18, 22, 24]. The physical properties that are mutual between the nanogels and the living tissues, are the consistency (soft and rubbery) and the low interfacial tension with water or biological fluids, which reduces the chances of a negative immune reaction (because protein adsorption and cell adhesion is minimized)[23]. Furthermore, they show a huge loading capacity of water-soluble compounds[13, 25]. They are an excellent reservoir for drugs, oligonucleotides and imaging agents, which is due to the porosity inside the crosslinked network that also protects their cargo from possible environmental degradation[24, 25]. Nanogels can have multifunctional properties that are dependent on their crosslinking density, chemical functional groups, and surface-active and stimuli-responsive constituents[24]. In fact, among other applications, nanogels have been used for drug delivery, but can also be applied in other fields such as sensing, diagnostics and bioengineering[26].

These nanocarriers present several advantages such as a three-dimensional (3D) tunable size and physical structure, a large surface area for multivalent bioconjugation, a network for the incorporation of biomolecules and biodegradability for a sustained drug release[3, 18, 22, 23]. In addition, nanogels also present flexibility and versatility, prolonged blood

circulation time and the option of being actively or passively targeted for a specific location, like tumor sites[27].

Some important issues in nanogel development must be considered. For example, their stability in biological fluids which is essential to avoid aggregation[13, 24]. It has been reported that nanogels with sizes around 100-200 nm have a higher cellular internalization efficiency, whereas small nanogels may result in a lower drug encapsulation and a fast drug release[13]. On the other hand, negatively charged nanogels are better in terms of resistance to protein interaction (they have a longer blood circulation half-life), while positively charged nanogels are more susceptible to interact with the serum components (which may cause aggregation and minimize the blood circulation half-life)[28]. Nevertheless, negatively charged nanogels may suffer repulsion by the negatively charged cell membrane, whereas the positively charged nanogels are more easily internalized by cells[28].

The combination of specific properties like targetability and stimuli-responsiveness can be used to create the perfect nanogel[29]. Indeed, nanogels have a characteristic which make them very interesting materials. They can be designed to be responsive to environmental stimuli like pH, temperature, ion strength or reduction agents (D,L-dithiothreitol (DTT), *etc*)[30], thus being an exceptional platform for biomedical applications.

1.4. Nanogels based on Alginate

Polysaccharides are known for their excellent physicochemical properties, biocompatibility and biodegradability[31]. Alginate is a linear polysaccharide composed of β–D-mannuronic acid and α–L-guluronic acid residues (Figure 2)[18, 27, 32-34]. It is a biocompatible and biodegradable natural polymer, extracted from marine brown algae or produced by bacteria[16, 33-35]. This polymer is considered safe by the U.S. Food and Drug Administration (FDA) for use in biomedical applications and is easily crosslinked in the presence of multivalent cations (calcium, barium, strontium, iron and aluminum) to form hydrogels which can be prepared at the nanoscale[32, 35-37]. Ionic crosslinking with calcium ions is the most used method to prepare alginate hydrogels and consists in the combination of an aqueous alginate solution with a solution of divalent calcium cations[34]. It is believed that the divalent cations bind to the guluronic blocks of the alginate chains, and form junctions in the polymer resulting in a gel structure[34].

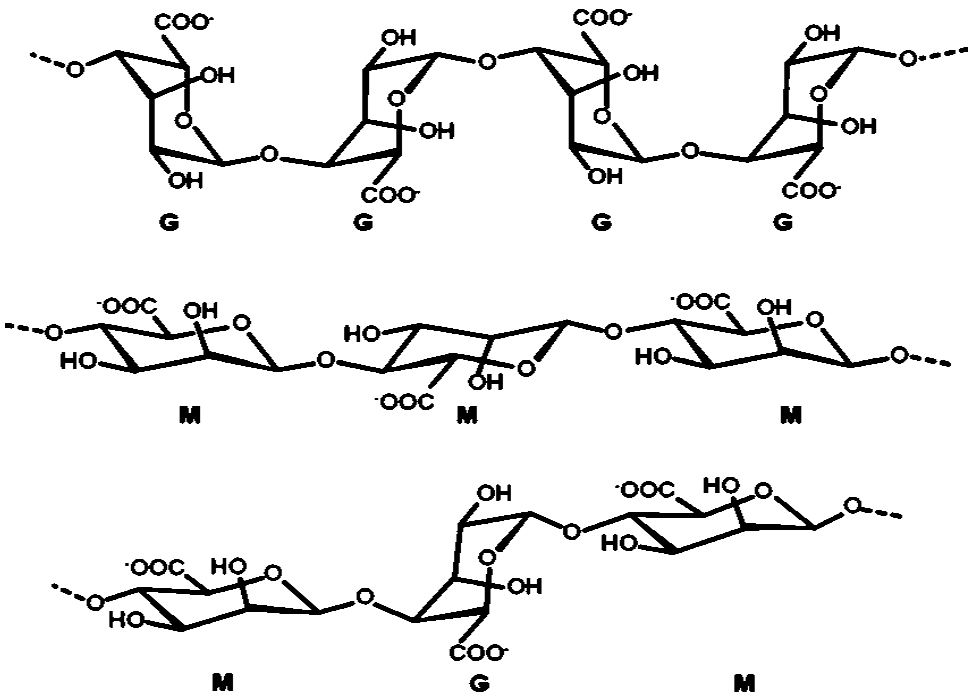

Figure 2. Structure of the β–D-mannuronic acid (M block) and α–L-guluronic acid (G block) residues, and the alternating blocks in alginate (adapted from reference 34).

As a consequence of the negative charge of its residues, alginate has a high degree of aqueous solubility, and a tendency for gelation under suitable conditions giving rise to nontoxic gels with a high porosity, low immunogenicity, and flexible to random geometries [27, 37]. Alginate nanogels have many biomedical applications due to their exceptional properties, being able to deliver bioactive peptides and proteins, genes, and small drugs. Alginate macro or microgels can even encapsulate living cells, such as fibroblasts, human mesenchymal stem cells (hMSC), or others [16, 32]. Beyond these applications, alginate can also be used in scaffolds for protein immobilization, and for neural, bone and cartilage tissue engineering[34, 37]. However, ionic crosslinked alginate nanogels usually exhibit poor mechanical properties, uncontrolled degradation under the physiological conditions and a burst drug release because of cation exchange in the biological medium (*e.g.*, exchange of calcium ions for sodium ions)[36]. The use of an anionic surfactant, like dioctyl sodium sulfosuccinate (AOT), can overcome this limitation, through the formation of a bilayer around alginate nanogels, producing a sustained release of the drug[36]. Another method to improve alginate based nanogel properties is through covalent crosslinking (*e.g.*, by the reaction of the hydroxyl and carboxylic acid functional groups) with reactive groups present in crosslinking reagents, for example through carbodiimide chemistry[35].

1.5. Stimuli-responsive nanogels

Stimuli-responsive nanogels are known to be sensitive/responsive when exposed to external signals, such as physical or chemical changes of the environment, are capable of changing their behavior. They are also named as "environment sensitive", "smart" or "intelligent" polymers[27, 29, 31]. These nanogels are able of controlled drug release *in vivo* when a specific stimuli is triggered in the target site[21]. The response of nanogels to changes in the environment may be physical (*e.g.*, variations in solubility, macromolecular structure, surface properties, swelling, and disassembly) or even a chemical reaction[29, 38]. The external signals can be also classified in physical signals (such as changes in temperature, electric or magnetic fields, and mechanical stresses (ultrasound)), and chemical signals (such as changes in pH, ionic strength, and concentration of specific molecules like enzymes or reducing agents) (demonstrated in Figure 3)[10, 29, 31, 39]. The release profile of the nanogels can be regulated by the stimuli-responsive units that are incorporated in the nanogel network[24].

Dual responsive nanogels can also be prepared and, in fact, nanogels sensitive to pH and temperature variations have been widely studied[30, 39, 40]. Nanogels that are simultaneously sensitive to pH and redox potential have been also reported[41]. Indeed, although many different stimuli can be used to control the behavior of nanogels (in particular their drug release behavior), the pH, the temperature and the redox potential can be considered the most important.

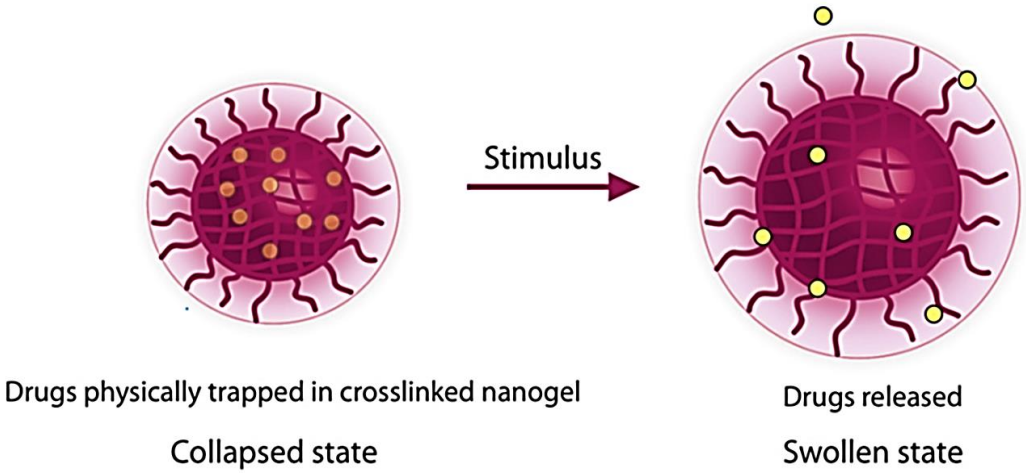

Figure 3. Behavior of nanogels with temperature, pH or other stimuli. *e.g.* the nanogel tend to swallow at lower temperature and shrink/collapse at higher temperature (adapted from reference 26).

pH-responsive nanogels

It is well known that the extracellular environment of solid tumors may exhibit an acidic pH value (around 6.5)[3], whereas normal tissues present a pH around 7.4[31, 41]. Furthermore, even more acidic pH values can be found in the human body, like in some intracellular compartments (endosomes and lysosomes presents a pH between 5.0 to 5.5)[3, 29]. For this reason, efforts have been done to develop pH-responsive nanogels that are stable at physiological pH but reacts to pH changes towards lower values for a more efficient delivery of small drugs, nucleic acids or proteins in target sites[29, 31]. pH-responsive polymers can be classified into two categories: polymers with ionizable groups, and polymers with degradable linkages[24, 31]. In the first category, polymers having weak acid or base groups, such as carboxylic acids, phosphoric acids and amines, can present a change in the ionization state by varying the pH[31]. The nanogels made from these polymers show an accelerated drug release that can be controlled through disassembly or dissolution[29, 31]. These polymers also have an important characteristic which is the ability to dissociate and associate with protons in the aqueous environment, and therefore can be used as proton donors or acceptors[29, 40]. The second category includes polymers that contain acid-degradable linkages[31]. The nanogels made from these polymers may suffer induced cleavage in acidic conditions that results in an increase of the porosity and, possibly, further polymer dissolution[31].

In response to changes in pH, nanogels based on polymers with ionizable groups go through a volume deformation[40]. When the pH of the solution is higher than the pK_a of the nanogel, *e.g.* poly(acrylic acid), the carboxylic groups are deprotonated carrying a negative charge, and resulting in the swelling of the nanogel. If these nanogels are loaded with hydrophilic drugs, then the swallow will result in a controlled drug release into the external medium. However, when the pH is lower than the pK_a of the nanogel, the carboxylic groups are protonated shrinking the nanogel[40].

The applications of pH-responsive nanogels in drug delivery is very important and, in particular, in the delivery of anticancer therapeutics.

Thermoresponsive nanogels

Thermoresponsive (or temperature-responsive nanogels) are prepared from thermosensitive polymers. These polymers show a temperature-dependent phase transition in solution, passing through a critical temperature known as critical solution temperature (CST)

[29]. For biomedical applications the transition temperature of the polymers should be between 10-40ºC to be effective[17]. If a polymer is water soluble below a defined temperature value and exists as a separated phase above that value, then it shows a lower critical solution temperature (LCST). If a polymer reveals the opposite behavior, then it shows an upper critical solution temperature (UCST)[29].

The most studied thermoresponsive polymer is poly(*N*-isopropylacrylamide), PNIPAM. Since it was first reported in 1968, PNIPAM is extensively used in biomaterials, bioconjugates, actuators, and sensors[17]. This polymer present a LCST about 32ºC because it goes through a reversible phase transition in water, from a swollen state (below 32ºC) to a collapsed state (above 32ºC)[29, 39, 40, 42, 43]. By showing this behavior, it can be used to incorporate hydrophilic and hydrophobic molecules[17, 29, 30, 39, 40, 42, 44] that are released in response to temperature changes (PNIPAM hydrogels present a reversible swelling-deswelling behavior)[13]. At 32ºC, PNIPAM becomes insoluble in water, shrinking, due to a disruption of the hydrogen bonds formed between NIPAM units and water molecules[17, 30, 39]. With these features, thermoresponsive nanogels with PNIPAM may have very interesting and promising applications in the biomedical field, like the treatment of certain cancers through hyperthermia[45]. They can be loaded with an anticancer drug and, at the target location, by moderately increasing the temperature above the LCST, the nanogel can change of volume and the drug release can be accelerated[13, 29].

Redox-sensitive nanogels

The intracellular and the extracellular environment have a huge difference in terms of reduction potential, and that is being explored for triggering the intracellular delivery of drugs[41]. For example, a reductive environment, such as the presence of an excess of glutathione (GSH), could be a powerful stimulus for drug delivery in the case of nanogels containing reducible bonds, such as disulfide bonds[28]. Actually, it was reported that the cytosol of cancer cells has a concentration of GSH around 2-10 mM, which corresponds to 1000 times more than that existent in the extracellular fluids, that presents a concentration between 2-20 μM[3, 11, 41, 46, 47]. So, the presence of GSH in the cytosol can promote the cleavage of disulfide bonds existent in nanogels and help the release of the encapsulated drugs when using DDS[11, 28]. On the other side, because of the low GSH concentration, the disulfide linkages should be stable in the circulation in normal physiological conditions[41]. It was reported that endolysosomes contain a high concentration of the reducing enzyme γ-

interferon-inducible lysosomal thiol reductase (GILT) and also of cysteine, both possibly contributing for a strong reducible environment[48].

1.6. General objectives of the thesis

The main goal of this thesis was to develop alginate (AG)-based nanogels for anticancer drug delivery with cell-responsiveness and/or sustained drug delivery behavior. The anticancer drug used in this study was Doxorubicin (Dox), a model drug extensively used to treat several types of cancers.

In more detail:

a) The first objective (Chapter II) was to prepare biocompatible redox-responsive nanogels based on disulfide-linked AG for intracellular delivery of Dox. The reducible nanogels were obtained through *in situ* crosslinking of AG by cystamine (Cys) *via* a miniemulsion method. The nanogels were characterized by Fourier transformed infrared spectroscopy (FTIR), dynamic light scattering (DLS), zeta potential measurements and scanning electron microscopy (SEM). Dox was loaded into the nanogels by simply mixing in aqueous solution, and the *in vitro* drug release was studied under normal and reductive conditions by UV-Vis spectroscopy. The antitumor activity was quantitatively and qualitatively studied against CAL-72 cells (an osteosarcoma cell line) using a cell metabolic activity assay and fluorescence microscopy, respectively.

b) The second goal (Chapter III) was to develop AG nanogels with dual crosslinking for improved sustained drug delivery. The nanogels were prepared through an emulsion method using calcium ions and cationic poly(amidoamine) (PAMAM) dendrimers of generation 5 (G5) as crosslinkers. Furthermore PAMAM dendrimers were conjugated with fluorescein isothiocyanate (FI), a fluorescent marker, for following the path of nanogels once inside cells. The characterization techniques involved nuclear magnetic resonance (NMR), dynamic light scattering (DLS), zeta potential measurements and scanning electron microscopy (SEM).

The *in vitro* drug release was studied by UV-Vis spectroscopy and the biological assays (antitumor activity of the Dox loaded nanogels and their tracking inside cells) were performed using CAL-72 cells (an osteosarcoma cell line) and NIH 3T3 fibroblasts (a non-carcinogenic cell line, used as a model of normal cells). Also in this case, quantitatively and qualitatively results were obtained through a cell metabolic activity assay and fluorescence microscopy, respectively.

References

1. Kumar A, Chen F, Mozhi A, Zhang X, Zhao Y, Xue X*, et al.* Innovative pharmaceutical development based on unique properties of nanoscale delivery formulation. Nanoscale. 2013;5:8307-8325.

2. Berindan-Neagoe I, Braicu C, Craciun L, Irimie A, Takahashi Y. Nanopharmacology in translational hematology and oncology. Int J Nanomed. 2014;9:3465-3479.

3. Wen Y, Oh JK. Dual-stimuli reduction and acidic pH-responsive bionanogels: intracellular delivery nanocarriers with enhanced release. RSC Adv. 2014;4:229-237.

4. del Valle EMM, Galán MA, Carbonell RG. Drug Delivery Technologies: The Way Forward in the New Decade. Ind Eng Chem Res. 2009;48: 2475–2486.

5. Verma G, Hassan PA. Self assembled materials: design strategies and drug delivery perspectives. Phys Chem Chem Phys. 2013;15:17016-17028.

6. Baguley BC. Multiple drug resistance mechanisms in cancer. Mol Biotechnol. 2010;46:308-316.

7. Vashist A, Vashist A, Guptac YK, Ahmad S. Recent advances in hydrogel based drug delivery systems for the human body. J Mater Chem B. 2014;2:147-166.

8. Park K, Mrsny RJ. Controlled Drug Delivery: Present and Future. Park K, Mrsny RJ, editors. In: Controlled Drug Delivery. 752. United States of America: American Chemical Society; 2000. p. 2-12.

9. Khandare J, Calderon M, Dagia NM, Haag R. Multifunctional dendritic polymers in nanomedicine: opportunities and challenges. Chem Soc Rev. 2012;41:2824-2848.

10. Gao W, Chan JM, Farokhzad OC. pH-Responsive Nanoparticles for Drug Delivery. Mol Pharmaceutics. 2010;7:1913-1920.

11. Liu J, Detrembleur C, Hurtgen M, Debuigne A, De Pauw-Gillet M-C, Mornet S*, et al.* Reversibly crosslinked thermo- and redox-responsive nanogels for controlled drug release. Polym Chem. 2014;5:77-88.

12. Zhang L, Li Y, Yu JC. Chemical modification of inorganic nanostructures for targeted and controlled drug delivery in cancer treatment. J Mater Chem B. 2014;2:452-470.

13. Qian Z-Y, Fu S-Z, Feng S-S. Nanohydrogels as a prospective member of the nanomedicine family. Nanomedicine. 2013;8:161-164.

14. Ang CY, Tan SY, Zhao Y. Recent advances in biocompatible nanocarriers for delivery of chemotherapeutic cargoes towards cancer therapy. Org Biomol Chem. 2014;12:4776-4806.

15. Sarker B, Papageorgiou DG, Silva R, Zehnder T, Gul-E-Noor F, Bertmer M*, et al.* Fabrication of alginate–gelatin crosslinked hydrogel microcapsules and evaluation of the microstructure and physico-chemical properties. J Mater Chem B. 2014;2:1470-1482.

16. Higham AK, Bonino CA, Raghavan SR, Khan SA. Photo-activated ionic gelation of alginate hydrogel: real-time rheological monitoring of the two-step crosslinking mechanism. Soft Matter. 2014;10:4990-5002.

17. Moon HJ, Ko du Y, Park MH, Joo MK, Jeong B. Temperature-responsive compounds as *in situ* gelling biomedical materials. Chem Soc Rev. 2012;41:4860-4883.

18. Oh JK, Lee DI, Park JM. Biopolymer-based microgels/nanogels for drug delivery applications. Prog Polym Sci. 2009;34:1261-1282.

19. Nicolas J, Mura S, Brambilla D, Mackiewicz N, Couvreur P. Design, functionalization strategies and biomedical applications of targeted biodegradable/biocompatible polymer-based nanocarriers for drug delivery. Chem Soc Rev. 2013;42:1147-1235.

20. Weinberg BD, Patel RB, Exner AA, Saidel GM, Gao J. Modeling doxorubicin transport to improve intratumoral drug delivery to RF ablated tumors. J Control Release. 2007;124:11-19.

21. Fu Y, Kao WJ. Drug release kinetics and transport mechanisms of non-degradable and degradable polymeric delivery systems. Expert Opin Drug Deliv. 2010;7:429-444.

22. Oh JK, Drumright R, Siegwart DJ, Matyjaszewski K. The development of microgels/nanogels for drug delivery applications. Prog Polym Sci. 2008;33:448-477.

23. Wu W, Zhou S. Hybrid micro-/nanogels for optical sensing and intracellular imaging. Nano Reviews. 2010;1:5730.

24. Yallapu MM, Jaggi M, Chauhan SC. Design and engineering of nanogels for cancer treatment. Drug Discov Today. 2011;16:457-463.

25. Moya-Ortega MD, Alvarez-Lorenzo C, Concheiro A, Loftsson T. Cyclodextrin-based nanogels for pharmaceutical and biomedical applications. Int J Pharm. 2012;428:152-163.

26. Chacko RT, Ventura J, Zhuang J, Thayumanavan S. Polymer nanogels: A versatile nanoscopic drug delivery platform. Adv Drug Deliver Rev. 2012;64:836-851.

27. Hamidi M, Azadi A, Rafiei P. Hydrogel nanoparticles in drug delivery. Adv Drug Deliv Rev. 2008;60:1638-1649.

28. Guo X, Shi C, Yang G, Wang J, Cai Z, Zhou S. Dual-Responsive Polymer Micelles for Target-Cell-Specific Anticancer Drug Delivery. Chem Mater. 2014;26:4405-4418.

29. Li Y, Dong H, Wang K, Shi D, Zhang X, Zhuo R. Stimulus-responsive polymeric nanoparticles for biomedical applications. Sci China Chem. 2010;53:447-457.

30. Peng J, Qi T, Liao J, Fan M, Luo F, Li H*, et al.* Synthesis and characterization of novel dual-responsive nanogels and their application as drug delivery systems. Nanoscale. 2012;4:2694-2704.

31. Binauld S, Stenzel MH. Acid-degradable polymers for drug delivery: a decade of innovation. Chem Commun. 2013;49:2082-2102.

32. Li Y, Rodrigues J, Tomás H. Injectable and biodegradable hydrogels: gelation, biodegradation and biomedical applications. Chem Soc Rev. 2012;41:2193-2221.

33. Coviello T, Matricardi P, Marianecci C, Alhaique F. Polysaccharide hydrogels for modified release formulations. J Control Release. 2007;119:5-24.

34. Lee KY, Mooney DJ. Alginate: properties and biomedical applications. Prog Polym Sci. 2012;37:106-126.

35. Jejurikar A, Seow XT, Lawrie G, Martin D, Jayakrishnan A, Grøndahl L. Degradable alginate hydrogels crosslinked by the macromolecular crosslinker alginate dialdehyde. J Mater Chem. 2012;22:9751-9758.

36. Vrignaud S, Benoit JP, Saulnier P. Strategies for the nanoencapsulation of hydrophilic molecules in polymer-based nanoparticles. Biomaterials. 2011;32:8593-8604.

37. Zhao W, Jin X, Cong Y, Liu Y, Fu J. Degradable natural polymer hydrogels for articular cartilage tissue engineering. J Chem Technol Biot. 2013;88:327-339.

38. Cao Z, Ziener U. Synthesis of nanostructured materials in inverse miniemulsions and their applications. Nanoscale. 2013;5:10093-10107.

39. Pasparakis G, Vamvakaki M. Multiresponsive polymers: nano-sized assemblies, stimuli-sensitive gels and smart surfaces. Polym Chem. 2011;2:1234-1248.

40. Lim HL, Hwang Y, Kar M, Varghese S. Smart hydrogels as functional biomimetic systems. Biomater Sci. 2014;2:603-618.

41. Chen J, Qiu X, Ouyang J, Kong J, Zhong W, Xing MM. pH and reduction dual-sensitive copolymeric micelles for intracellular doxorubicin delivery. Biomacromolecules. 2011;12:3601-3611.

42. Doring A, Birnbaum W, Kuckling D. Responsive hydrogels - structurally and dimensionally optimized smart frameworks for applications in catalysis, micro-system technology and material science. Chem Soc Rev. 2013;42:7391-7420.

43. Schmaljohann D. Thermo- and pH-responsive polymers in drug delivery. Adv Drug Deliv Rev. 2006;58:1655-1670.

44. Chiang WH, Ho VT, Huang WC, Huang YF, Chern CS, Chiu HC. Dual stimuli-responsive polymeric hollow nanogels designed as carriers for intracellular triggered drug release. Langmuir. 2012;28:15056-15064.

45. Quan CY, Sun YX, Cheng H, Cheng SX, Zhang XZ, Zhuo RX. Thermosensitive P(NIPAAm-co-PAAc-co-HEMA) nanogels conjugated with transferrin for tumor cell targeting delivery. Nanotechnology. 2008;19:275102.

46. Zhu J, Shi X. Dendrimer-based nanodevices for targeted drug delivery applications. J Mater Chem B. 2013;1:4199-4211.

47. Wang X, Cai X, Hu J, Shao N, Wang F, Zhang Q*, et al.* Glutathione-triggered "off-on" release of anticancer drugs from dendrimer-encapsulated gold nanoparticles. J Am Chem Soc. 2013;135:9805-9810.

48. Cheng R, Feng F, Meng F, Deng C, Feijen J, Zhong Z. Glutathione-responsive nano-vehicles as a promising platform for targeted intracellular drug and gene delivery. J Control Release. 2011;152:2-12.

CHAPTER II. Redox-Responsive Alginate Nanogels with Enhanced Anticancer Cytotoxicity

***This Chapter is based on the following publication:**

Maciel D, Figueira P, Xiao S, Hu D, Shi X, Rodrigues J, Tomás H, Li Y. Redox-Responsive Alginate Nanogels with Enhanced Anticancer Cytotoxicity. Biomacromolecules. 2013;14:3140-3146. (Published)

Abstract

Although doxorubicin (Dox) has been widely used in the treatment of different types of cancer, its insufficient cellular uptake and intracellular release is still a limitation. Herein, we report an easy process for the preparation of redox-sensitive nanogels which were shown to be highly efficient in the intracellular delivery of Dox. The nanogels (AG/Cys) were obtained through *in situ* crosslinking of alginate (AG) using cystamine (Cys) as a crosslinker *via* a miniemulsion method. Dox was loaded into the AG/Cys nanogels by simply mixing it in aqueous solution with the nanogels, that is, by the establishment of electrostatic interactions between the anionic AG and the cationic Dox. The results demonstrated that the AG/Cys nanogels are cytocompatible, have a high drug encapsulation efficiency (95.2±4.7%), show an *in vitro* accelerated release of Dox in conditions that mimic the intracellular reductive conditions, and can quickly be taken up by CAL-72 cells (an osteosarcoma cell line), resulting in higher Dox intracellular accumulation, and a remarkable cell death extension when compared with free Dox. The developed nanogels can be used as a tool to overcome the problem of Dox resistance in anticancer treatments, and possibly be used for the delivery of other cationic drugs in applications beyond cancer.

Keywords: Doxorubicin; alginate; redox-sensitive nanogels; intracellular drug delivery

Introduction

Cancer is one of the most serious diseases around the world. Doxorubicin (Dox), one of the smallest anticancer drugs, has been widely used for chemotherapy of several kinds of cancers of different organs, including bone[1], liver[2, 3] or breast[4]. Dox is a member of the anthracycline family of anticancer drugs, and its use for cancer treatment can lead to a sequence of complications, such as tumor resistance, cellular toxicity and particularly cardiotoxicity[5]. In the other hand, Dox presents antitumor activity since it intercalates in the DNA double helix and, as a consequence, inhibits DNA replication and the biosynthesis of macromolecules[5, 6].

However, Dox is a weak base with a pK_a of 8.30 and tends to undergo ion trapping in acidic conditions of the extracellular microenvironment of solid tumors (pH of 6.5 to 6.9) and in the internal milieu of endolysosomes (pH of 5.0 to 5.5)[6, 7]. The ion trapping phenomenon is caused by the acidic regions of solid tumors creating a physiological barrier for the cellular uptake of weak bases, that are seized by acidic compartments, leading to drug resistance[7, 8]. This occurs when there is a big difference between the permeabilization of ionized and nonionized species of a drug[7].

Weak base drugs, such as Dox, ionize in solution, and an equilibrium is established between the protonated species with the uncharged, unprotonated form of the drug[8]. While uncharged Dox can freely permeate membranes, the protonated Dox has a lower membrane permeability becoming trapped inside acidic compartments. Furthermore, Dox has been reported to have multidrug resistance[9, 10], possibly because of the p-glycoprotein, also known as the multidrug resistance protein, that is responsible for pumping unfamiliar molecules out of the cell. Therefore, free Dox can likely be pumped out of the cells by p-glycoprotein which shows enhanced activity in acid environments[9]. Both these situations limit the therapeutic bioactivity of free Dox. So, to keep its desirable therapeutic efficacy, a large dosage or an increased number of injections may be needed which can lead to adverse side effects in normal tissues, especially in the heart and kidneys, causing heart failure and cardiomyopathy among others malignancies and thus limiting its clinical applications[10-13]. Due to these adverse effects, it is extremely important to develop biocompatible platforms for effective Dox delivery into the cytoplasm and/or the cell nucleus.

Encapsulating anticancer drugs into nanocarriers can be the answer. The encapsulation of drugs may reduce or avoid the toxicity associated to the free drug, sustain the drug release, enhance drug solubility and allow targetability to cancer cells and/or tumors

site *via* the Enhanced Permeation and Retention (EPR) effect[14-17]. Furthermore, the encapsulation of Dox inside nanocarriers can also protect it from recognition by the p-glycoprotein, resulting in an improved intracellular accumulation and Dox resistance reduction[18]. Cell-responsive nanocarriers, which are sensitive to intracellular microenvironmental stimuli, such as temperature[19], pH[20] and reduction potential[21], can be used as mean of controlling the drug release. After arrival in tumor tissues, these smart nanocarriers can be endocytosed by cells and release the loaded drug triggered by intracellular stimuli, consequently exerting maximal antitumor activity and minimal side effects to the body[22].

It is reported that the glutathione (GSH) concentration in the cytoplasm (about 2-10 mM) is about 1000 times higher than that in the extracellular environment (about 2-20 μM)[23]. Additionally, the GSH concentration in tumor cells is several times higher than in normal cells[24]. Protection and detoxification are some of the functions of GSH, which can be one of the reasons that explains the decrease in cytotoxicity of many chemotherapeutic agents[24]. It was also reported that endolysosomes contain a high content of a specific reducing enzyme γ-interferon-inducible lysosomal thiol reductase (GILT) and also of cysteine[23]. As such, disulfide bonds present in the nanocarriers will be easily degraded in this reducing environment, while remain more stable in the extracellular space with lower -SH concentration. The development of reducible nanosystems (containing -SH-cleavable disulfide bonds) for efficient delivery of antitumor drugs is a challenge for researchers[23-25].

Compared to other nanocarriers, such as liposomes[26, 27], micelles[28], dendrimers[29, 30] hydroxyapatite nanoparticles[31], and nanotubes[32, 33], nanogels show good biocompatibility, high aqueous dispersability and stability, well-defined structure and multifunctional possibilities[34, 35]. As a natural and nontoxic biodegradable polymer, alginate (AG) has been widely investigated for therapeutic applications[36]. AG is an anionic polymer that can form gels and encapsulate cationic molecules very effectively due to their high binding ability (through electrostatic interactions) and thus increased drug loading capacity[37]. Recently, calcium-crosslinked AG nanogels (Ca^{2+}-AG) have been fabricated and used for delivery of Dox with improved antitumor activity[38, 39]. However, pure Ca^{2+}-crosslinked AG nanogels have uncontrollable stability and often give a burst drug release, probably caused by the rapid exchange of Ca^{2+} with other cations present in phosphate buffered saline (PBS) solution[38, 40]. Additionally, only limited amount of Dox is released from Ca^{2+}-AG nanogels, which hampers the Dox antitumor efficacy[39]. Chang *et al.* synthesized oxidized sodium alginate and then thiolated it to get thiolated alginate (AG-SH), which then assembled into reducible AG

nanoparticles in water by oxidation of AG-SH in air [41]. However, the synthesis process was very complicated, and the AG-SH was difficultly stored due to its sensitivity to oxygen in air. Also, aggregation was a problem during the disulfide crosslinking process.

In this work, a simple approach was employed to develop biocompatible reduction-responsive nanogels based on disulfide-linked alginate for efficient intracellular delivery of Dox. The reducible nanogels with controllable size were synthesized through *in situ* crosslinking of alginate by cystamine *via* a miniemulsion method. The nanogels were shown to have excellent biocompatibility. Dox was loaded into the nanogels by simply mixing in aqueous solution, and the *in vitro* drug release was accelerated in intracellular reductive conditions. These Dox-loaded nanogels showed improved antitumor activity towards CAL-72 cells (an osteosarcoma cell line), compared to free Dox. This study is expected to be helpful for the design of more effective and safer nanogel-based drug carrier systems which may find applications in a wide range of fields.

Materials and Methods

Materials

Alginate acid sodium salt (from brown Algae, Mw from 12 to 58 kD, cell culture tested) (AG) was purchased from Sigma, USA. Cystamine dihydrochloride (Cys) was bought from Fluka. 1-Ethyl-3-(3-Dimethylamino propyl) carbodiiamide hydrochloride (EDC) was bought from J&K Chemical Ltd. Dioctyl sodium sulfosuccinate (AOT) was obtained from Sigma-Aldrich. Dichloromethane (DCM) HPLC grade was purchased from Fisher. Polyvinyl Alcohol (PVA, Mw 72000 Da) was bought from Merck, Germany. Doxorubicin hydrochloride (Dox) was obtained from Aldrich and used as received. D,L-Dithiothreitol (DTT) was purchased from Sigma Aldrich. CAL-72 cells were purchased DSMZ, Germany. 4', 6-Diamidino-2-phenyindole dilactate (DAPI) was bought from Sigma, USA. Glutaraldehyde was obtained from Merck, Germany. Dulbecco's phosphate buffer saline (PBS) (without Ca^{2+} and Mg^{2+}) was bought from Invitrogen Corporation, USA. All the other reagents were purchased from Sigma, unless otherwise stated.

Preparation and Characterization of the AG/Cys and AG/Cys-Dox Nanogels

AG nanoparticles were prepared by adapting a published double emulsion method[38, 39]. A total of 2 g of 1 wt% AG aqueous solution was dropped into 0.25 mL of ultrapure (UP) water with 5.5 mg EDC, followed by stirring at 400 rpm for 3 h at room temperature. The mixture was dropped into 4 mL of 2.5 wt% AOT solution in DCM under stirring at 1000 rpm. The mixture was stirred under 400 rpm for 5 min, and then was dropped into 30 g of 2 wt% PVA aqueous solution, followed by stirring at 400 rpm for 10 min. 50 mg of Cys in 1 mL UP water was dropped into the above solution, and then stayed overnight under stirring at 400 rpm for DCM evaporation. The obtained mixture was centrifuged (15000 rpm for 5 min) and washed with distilled water (25 mL x 3 times). The precipitate was freeze-dried for 3 days to get AG/Cys nanogels.

The AG/Cys-Dox nanogels were prepared according to Figure 4 by dropping 2 mg Dox in 1 mL water into 5 mL UP water containing 50 mg of AG/Cys. The mixture was kept overnight under magnetic stirring, followed by centrifuge to remove free Dox. The supernatant was determined spectrophotometrically at 490 nm using an ultraviolet-visible (UV-Vis) spectrometer (Lambda 2, Perkin-Elmer) for indirect determination of the Dox

encapsulation efficiency (EE). The analysis was performed based on a Dox calibration curve. The least-squares approach was used to fit the data (the regression equation and the correlation coefficient at 490 nm were y = 12611x + 0.0299 and 0.9979, respectively). The experimental molar absorption coefficient for Dox was 12611 M^{-1}. The precipitate was lyophilized and kept at 4 °C for further study.

The Fourier transform infrared (FTIR) spectra of AG and AG/Cys nanogels recorded on a Spectrometer (Spectrum Two, Perkin-Elmer) in a transmission mode ranging from 650 to 4000 cm^{-1} under ambient conditions.

The particle size and the zeta potential of the AG/Cys and AG/Cys-Dox nanogels were measured using a Zetasizer Nano ZS (Malvern Instruments) equipment. The nanogels were dispersed in PBS and sonicated for 15 min before measurements.

The morphology of the AG/Cys and AG/Cys-Dox nanogels were examined by scanning electron microscopy (SEM, JSM-5600LV, JEOL Ltd., Japan) with an operating voltage of 15 kV. Before measurement, the samples were dispersed in UP water under sonication (SK1200H, 50 W) for 10 min. The aqueous suspensions of the samples were dropped onto an aluminum foil, air-dried, and Au-sputtered coated before analysis.

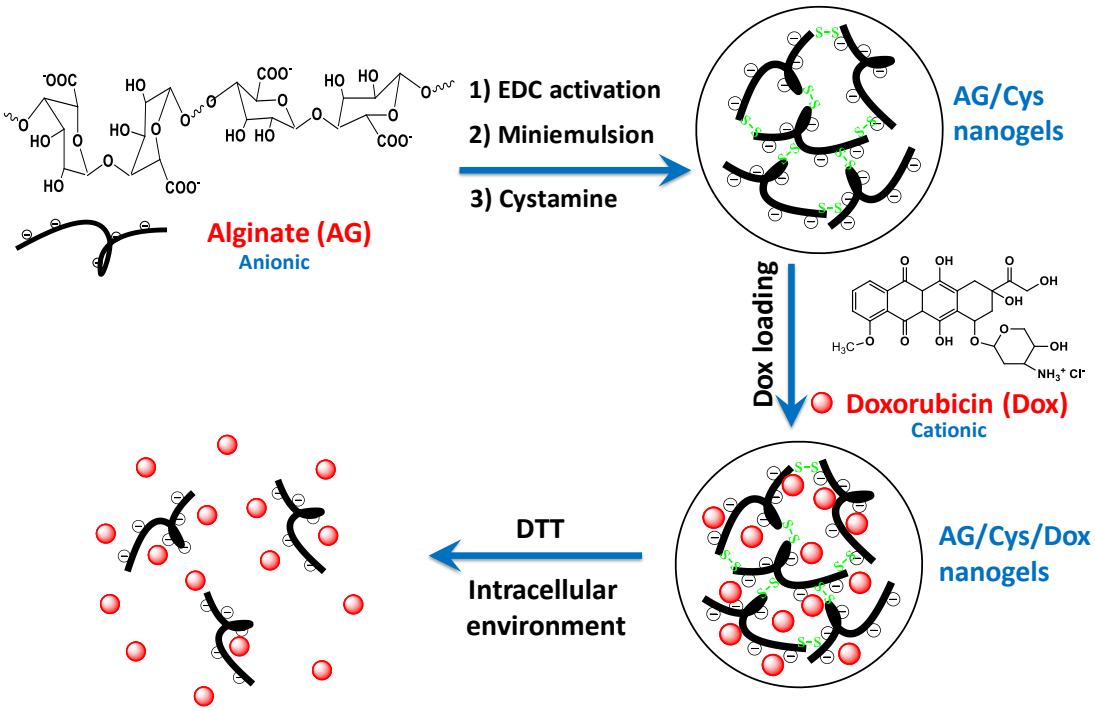

Figure 4. Schematic illustration of the formation and drug release of Dox-loaded (AG/Cys-Dox) nanogels.

In vitro drug release studies

In triplicate, 1 mg of AG/Cys-Dox nanogels was dispersed in 2 mL of PBS at 37 ºC under a pH value of 7.4, in the absence and presence of 5 mM DTT. At different time intervals, the solutions were centrifuged at 12000 rpm for 5 min. The supernatants were analyzed spectrophotometrically at 490 nm using an UV-Vis spectrometer for the Dox release analysis. The cumulative release (*Cr*) of Dox against time was obtained according to the equation:

$$Cr = 100 * \frac{Abs_t}{Abs_{tot}} \qquad (1)$$

Where Abs_t and Abs_{tot} are the cumulative amount of drug released at time *t* and total drug contained in the nanogels used for drug release, respectively.

Cell Biological Evaluation

CAL-72 cells (an osteosarcoma cell line) were cultured in Dulbecco's Modified Eagle Medium (D-MEM) containing 10% (v/v) fetal bovine serum (FBS, Gibco) and 1% (v/v) of an antibiotic-antimycotic 100x solution (AA, Gibco, with penicillin, streptomycin, and amphotericin B). The medium was supplemented with 1% (v/v) of L-glutamine 100x solution (Gibco) and 1% (v/v) of insulin-transferin-selenium 100x solution (ITS, Gibco). The cells were grown at 37ºC, in a humidified atmosphere, in an atmosphere of 5% carbon dioxide. Afterwards, the cells were harvested at 70-80% confluence, using trypsin-EDTA solution for the enzymatic detachment of the cells from the plastic substrate.

For the cytotoxicity experiments, CAL-72 cells were first plated in 24-well plate for 24 h at a seeding density of 16 x 10^3 cells per well. After one day, free Dox and AG/Cys-Dox nanogels solutions (with equivalent Dox concentrations), prepared in PBS buffer, were added to the cell culture media and then incubated for 48 h at 37ºC before the resazurin reduction assay. Solutions of PBS and AG/Cys nanogels in PBS (containing equivalent mass concentrations to those used in AG/Cys-Dox nanogel solutions) were used as controls.

The cell viability was quantified by the measurement of the metabolic activity of the cells in the culture through the resazurin reduction assay. Briefly, after the 48 h incubation time, the cell culture medium was replaced with fresh medium containing resazurin at a concentration of 0.1 mg/mL and kept at 37ºC for 3 h. Afterward, aliquots of the cell supernatant were transferred to 96-well opaque plates and the resofurin fluorescence (λ_{ex}=530

nm, λ_{em}=590 nm) was measured using a microplate reader (model Victor^3 1420, Perkin-Elmer). Statistical analysis was performed using the IBM SPSS Statistics 20 software (IBM Inc., Armonk). One-way ANOVA with Tukey Post Hoc test was used to assess the statistical difference between group means.

For the cell uptake study, cells were plated 24 h before the incubation, to allow the attachment. In these experiments, solutions of free Dox and AG/Cys-Dox nanogels were used at the same Dox concentration (the final concentrations in the wells were 0.5 μM). Cells were then incubated with the test solutions at 37ºC for 2 and 4 h. Subsequently, the cultures were washed with sterilized PBS buffer, fixed with 3.7% glutaraldehyde, stained with DAPI for 30 min, and visualized using a fluorescence microscope (Nikon Eclipse TE 2000E).

Results and Discussion

Preparation and Physical Characterization of AG/Cys-Dox Nanogels

Initially, an aqueous solution of AG was reacted with EDC to activate the AG carboxylic groups. The mixture was emulsified in DCM using AOT as surfactant. The obtained mixture was re-emulsified in a PVA aqueous solution, followed by the addition of Cys to crosslink AG-emulsified drops. The reaction rested overnight to evaporate the organic DCM, and was then centrifuged and washed with water to remove the remaining surfactants and side products. The final precipitate was lyophilized to obtain the disulfide-cross-linked nanogels (AG/Cys), as is illustrated in Figure 4.

The AG/Cys nanogels were prepared and loaded with Dox in aqueous solution. The strong electrostatic interactions between the nanogels and Dox were taken in advantage in the formation of the Dox-loaded nanogels. The addition of Dox only in the second step of the production process was done to avoid the possible nondegradable chemical bond formation between the EDC-activated carboxylic acid groups on AG and the amino group of Dox (this would limit the Dox release efficiency and lower its bioactivity). Having this in mind, the procedure followed is different from the nanogels by ionic crosslinking that is the case where the drug is added to the initial AG solution[38, 39].

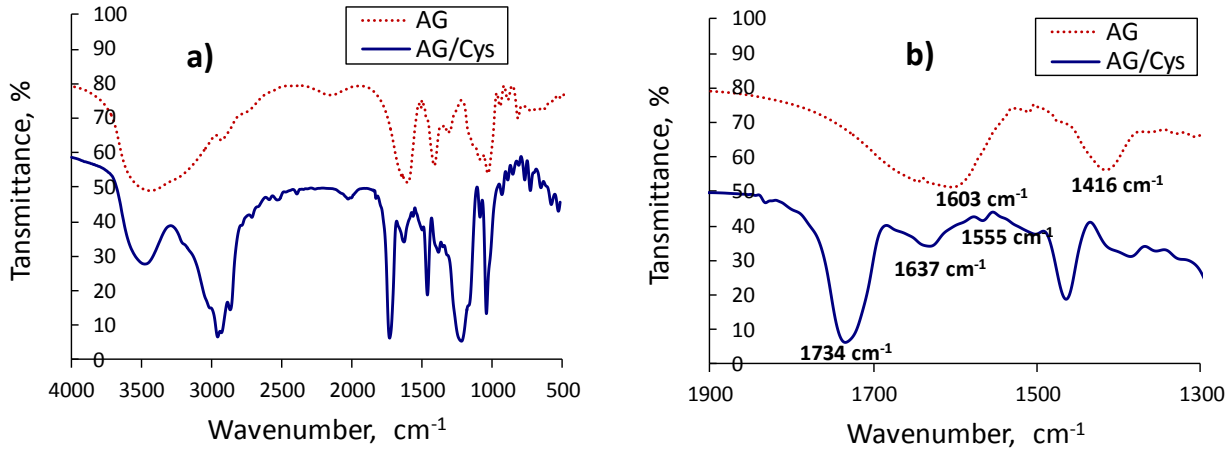

Figure 5. FTIR spectra of pure AG and AG/Cys nanogels (a); (b) is an enlarged view of the spectra in the range of 1300 to 1900 cm^{-1}.

The chemical structure of AG and AG/Cys was further characterized by Fourier Transform Infrared (FTIR) analysis. As can be seen in Figure 5, AG presents the characteristic FTIR spectrum of its polysaccharide structure, with broad peaks around 3434

cm^{-1} (the hydroxyl stretching vibration of the polysaccharide), and large absorption bands at 1603 and 1416 cm^{-1} (asymmetric and symmetric stretching peaks of the carboxylate salt groups)[42]. After the crosslinking reaction of AG with Cys, the intensity of the peaks at 1603 and 1416 cm^{-1} was greatly reduced, and the peaks shifted to 1637 cm^{-1} (C=O stretching (amide I)) and 1555 cm^{-1} (NH in-plane bending (amide II))[43-45], indicating the formation of amide bonds between AG and Cys. The new peak at 1734 cm^{-1} of AG/Cys might be associated with the ester linkage (C=O stretching) of the surfactant, AOT, which can still remain in the nanogels[46].

Dox is widely employed in the treatment of different types of tumors, as this molecule can bind DNA and block the synthesis of bioactive macromolecules[5]. To better understand the potential applications of the obtained nanogels for drug delivery, Dox was selected as a model drug and used in the study of their loading and release properties. Dox-loaded AG/Cys nanogels (AG/Cys-Dox) were obtained *via* electrostatic interaction by simply mixing aqueous solutions of cationic Dox and of anionic AG/Cys nanogels. Subsequently, free Dox was removed by centrifugation, and the supernatant was analyzed with UV−visible spectrometer at 490 nm wavelength to determine the amount of unencapsulated Dox. As shown in Table 1, the AG/Cys nanogels presented high Dox encapsulation efficiency (95.2 ± 4.7%) and high loading capacity (3.7 ± 0.2%), revealing the successful loading of the drug and electrostatic binding to AG. Thereby, nanogels with a disulfide-cross-linked three-dimensional structure were prepared and can effectively serve as a drug reservoir for cationic Dox.

Table 1. Characterization of Dox-loaded AG/Cys Nanogels[1]

Sample	Size, nm[b]	Zeta Potential, mV	EE, %[c]	LC, %[d]
AG/Cys	207 ± 47	-62 ± 11	---	---
AG/Cys-Dox	318 ± 62	-39 ± 11	95.2 ± 4.7	3.7 ± 0.2

[1]The results are expressed as the mean±standard deviation (n = 3). [b]Size and zeta potential were measured in PBS at pH 7.4. [c]Encapsulation efficiency = 100 x W_t/W_0, W_0 and W_t are the total Dox weight used for encapsulation and the weight of encapsulated Dox, respectively. [d]Loading Capacity = 100 x W_t/W , W_t and W are the weight of encapsulated Dox and the weight of Dox-loaded nanogels, respectively.

Table 1 shows the hydrodynamic diameter (size) of the nanogels analyzed by dynamic light scattering (DLS) and the correspondent zeta potentials. The zeta potential appeared to display an increase from −42 ± 11 mV (AG/Cys) to −39 ± 11 mV (AG/Cys-Dox) in PBS (pH 7.4) after the Dox encapsulation. Because of their hydrophilicity and negatively charged surface, the nanogels are expected to be very stable in physiological conditions. The size of AG/Cys was 207 ± 47 nm, which indicated that the nanogels were well dispersed in physiological buffer, while AG/Cys-Dox had a bigger size (318 ± 62 nm) than AG/Cys. The increase of size in the AG/Cys-Dox together with its likely increase in zeta potential indicates that Dox was successfully loaded into AG/Cys nanogels to form nanocomplexes. It is important to refer that the Dox-loaded nanogels can be lyophilized and redispersed very well in physiological buffer that can be confirmed by DLS analysis, which is an important factor for therapeutic formulations for long-term storage.

The scanning electron microscopy (SEM) images for the two kinds of samples are shown in Figure 6. SEM micrographs indicate that AG/Cys are present as dispersed nanoparticles with a size ranging from 100 to 250 nm, which is in agreement with the results of DLS analysis. The loading of Dox into the AG/Cys does not appear to have affected the size of the nanogels (Figure 6b). It has to be mentioned that SEM micrographs reflect the dry state of materials. The higher hydrodynamic diameter of the AG/Cys-Dox than that of the Dox-free nanogels may be ascribed to the incorporation of the hydrophilic Dox, probably resulting in a more swollen state in PBS solution.

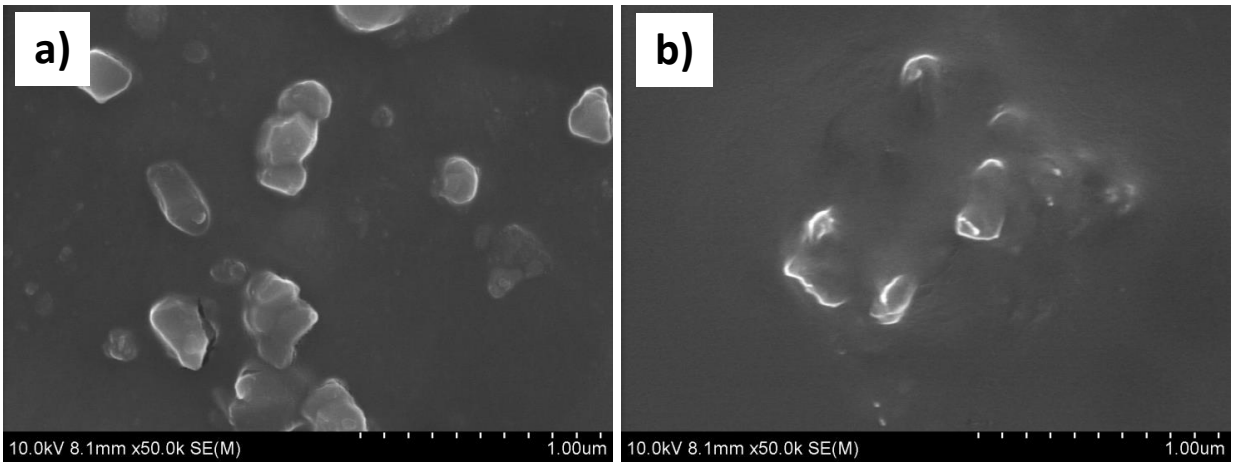

Figure 6. Scanning electron microscope (SEM) images of the AG/Cys (a) and AG/Cys-Dox (b) nanogels.

In Vitro Drug Release of Dox-Loaded Nanogels

The idea behind the design of these nanogels is that, after cellular uptake and in the presence of the intracellular reducible environment, the disulfide bonds can be cleaved to trigger the release of Dox into the cytosol and the nucleus (Figure 4). To check this hypothesis, the release behavior of Dox from the nanogels was studied in nonreducible and reducible environments, in PBS buffer, at pH 7.4. D,L-Dithiothreitol (DTT, 5 mM) was hereby applied as a reducing molecule to mimic the intracellular reducible environment and to examine the possible responsive release of the Dox loaded in the nanogels. As can be seen from Figure 7, after incubation in PBS for 30 min, a limited Dox amount (about 20.0 ± 3.2%) was released from the nanogels under normal physiological conditions (pH 7.4), whereas it was promptly enhanced (49.6 ± 3.3%) in the presence of 5 mM DTT. For both situations, the release process ended after 6 h, and final cumulative Dox releases of 23.1 ± 3.5% and 70.1 ± 1.6% were obtained, respectively, in the absence and in the presence of DTT. The drug release results clearly show that the nanogels have a reduction-triggered drug release behavior and destabilize in a medium mimicking the intracellular reductive environment.

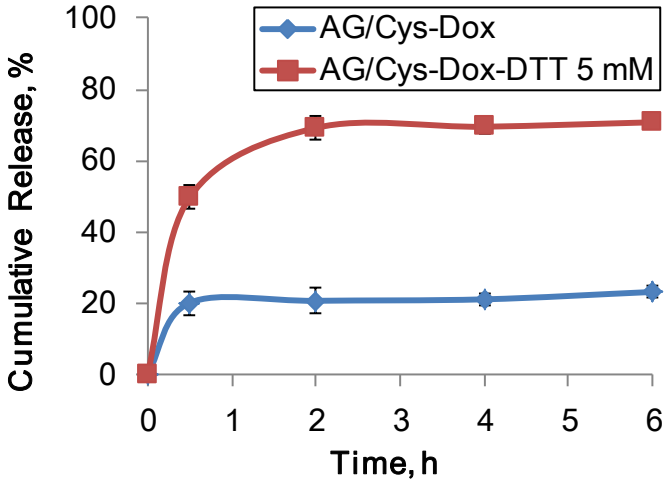

Figure 7. *In vitro* cumulative release of Dox from AG/Cys-Dox nanogels in the presence and absence of DTT (5 mM) in PBS buffer (pH 7.4) at 37°C. The results are expressed as the mean ± standard deviation (n = 3).

Therefore, after being internalized by cells through endocytosis and after endosome/lysosome merging, the disulfide bonds present in the nanogels will be cleaved by the action of molecules with reductive properties, such as the specific reducing enzyme γ-

interferon-inducible lysosomal thiol reductase (GILT) and cysteine, and undergo partial degradation. This accelerates the release of Dox from the nanogels which will reach the cytoplasm after endolysosomes rupture. Because the separation of Dox (positive) from the AG chains can be achieved through its substitution by protons (H^+), an increase in the influx of protons to the endolysosomes can occur and facilitate their rupture through the known "proton-sponge effect"[47]. Finally, reductive molecules existent in the cytoplasm, like glutathione (GSH), will further disassemble the redox-responsive nanogels, accelerate Dox release and allow the movement of Dox to the cell nucleus to kill cancer cells.

In Vitro Cytotoxicity of Nanogels and Dox-Loaded Nanogels

To evaluate the antitumor activity of Dox upon release from the nanogels, the *in vitro* cytotoxicity of Dox-loaded nanogels was tested using CAL-72 cells and the resazurin reduction assay. This assay is used as an indirect measure of cell viability because what is really being quantified is the cell metabolic activity (it is established a direct correlation between cell metabolic activity and the number of viable cells). Free Dox and AG/Cys nanogels were used as controls (as positive and negative controls, respectively). As shown in Figure 8, cell viability was dependent on Dox concentration. Both free Dox and AG/Cys-Dox nanogels were able to inhibit the growth of CAL-72 cells at all tested Dox concentrations (compared with the PBS control). Free Dox alone exhibited the expected mild drug resistance with an IC_{50} above 2.0 μM, while the Dox-loaded nanogels displayed a higher inhibition efficacy towards CAL-72 cells (with obvious reduction in IC_{50} (0.9 μM)). Because the Dox-free AG/Cys nanogels did not display any cytotoxicity, results indicate that the antitumor efficacy is specially related with the presence of Dox within the carriers. Actually, the cell viability of CAL-72 cells treated with AG/Cys nanogels for 48 h was above that obtained for the PBS control (100%), at all test concentrations (up to 30.4 μg/mL), which reveals that the nanogels even have a beneficial effect over the metabolic activity of the cells. The excellent cytocompatibility of the nanogels together with their efficacy as Dox carriers show that they have a high potential as platforms for the intracellular delivery of anticancer drugs.

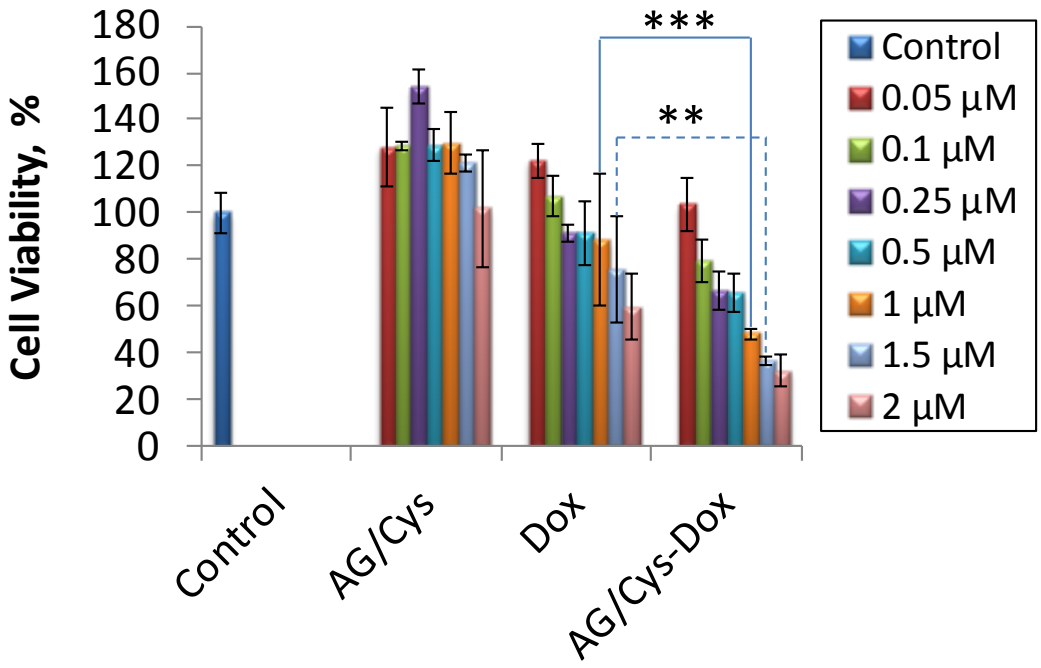

Figure 8. Cytotoxicity of free Dox, AG/Cys-Dox nanogels (with equivalent Dox concentration), and AG/Cys nanogels (with equivalent weight concentration of the corresponding AG/Cys-Dox nanogels) was analyzed after 48 h of cell culture using CAL-72 cells. Results are reported as the mean ± standard deviation (n = 4). One-way ANOVA with Tukey's Post Hoc test was used to assess the statistical difference between the group means (**$p < 0.01$, ***$p < 0.001$).

In order to confirm the antitumor activity of the nanogels, the morphology of cells treated for 48 h with free Dox, AG/Cys, and AG/Cys-Dox nanogels were observed by optical microscopy (Figure 9). Cells in the PBS control and those treated with AG/Cys nanogels exhibit a fusiform shape and are adherent on the cell dish surface, indicating that the AG/Cys nanogels are quite cytocompatible. At a Dox concentration of 0.5 µM, samples treated with free Dox have a portion of rounded and non-adherent cells, showing a moderate level of cytotoxicity. As a comparison, there are a high amount of rounded and non-adherent cells, and less quantity of fusiform and attached healthy cells, when AG/Cys-Dox nanogels containing 0.5 µM Dox were used, suggesting a larger cytotoxicity. The cell morphological results are in agreement with the quantitative analysis made by the resazurin reduction assay, showing that AG/Cys-Dox nanogels display a more efficient antitumor activity.

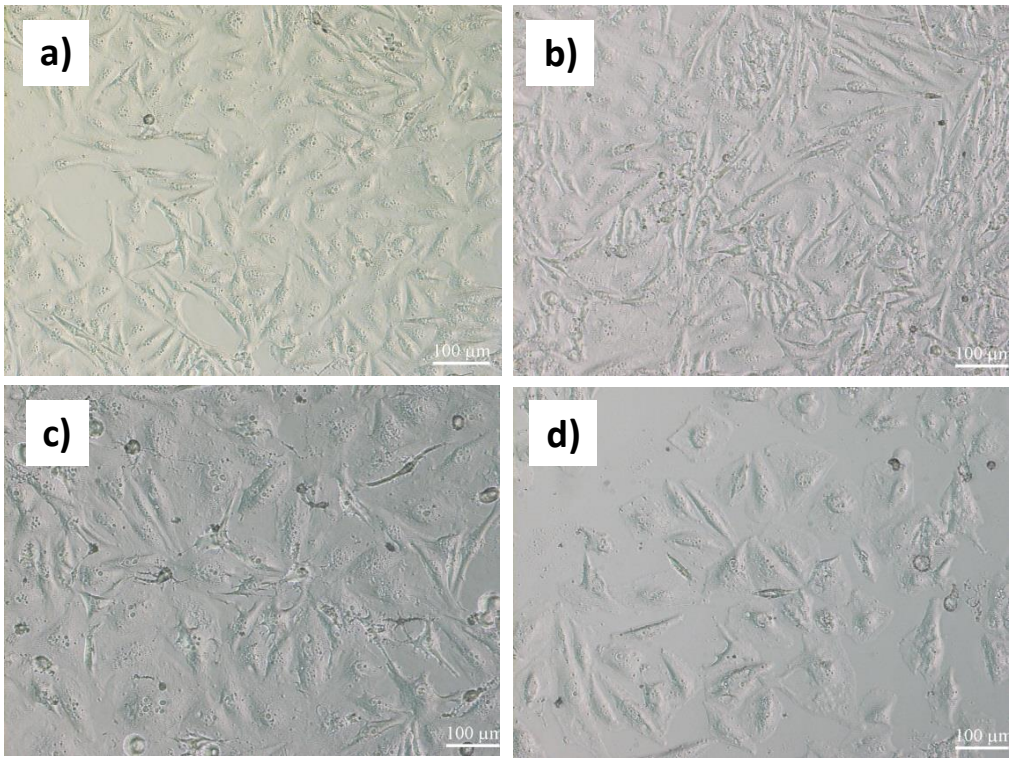

Figure 9. Cell morphology (optical microscopy) of CAL-72 cells after 48 h in culture with (a) control, (b) AG/Cys, (c) free Dox (0.5 µM), and (d) AG/Cys-Dox nanogels with an equivalent amount of Dox (0.5 µM).

Cellular Internalization of Doxorubicin

The uptake of the drug carriers by cells is one of the key factors for the achievement of therapeutic efficacy[48]. Since Dox is a fluorescent molecule (it emits red light), its cellular uptake can be easily followed by fluorescence microscopy. The red fluorescence of Dox could be observed inside CAL-72 cells after 2 h of incubation for both the experiments performed with free Dox and with Dox-loaded AG/Cys nanogels (Figure 10). After 2 and 4 h incubation, the red fluorescence of Dox was observed not only in the cytoplasm but also in the nucleus. The results further show that the fluorescence intensity was lower for the experiments done in the presence of free Dox, than for those done using Dox-loaded AG/Cys nanogels (Figure 10).

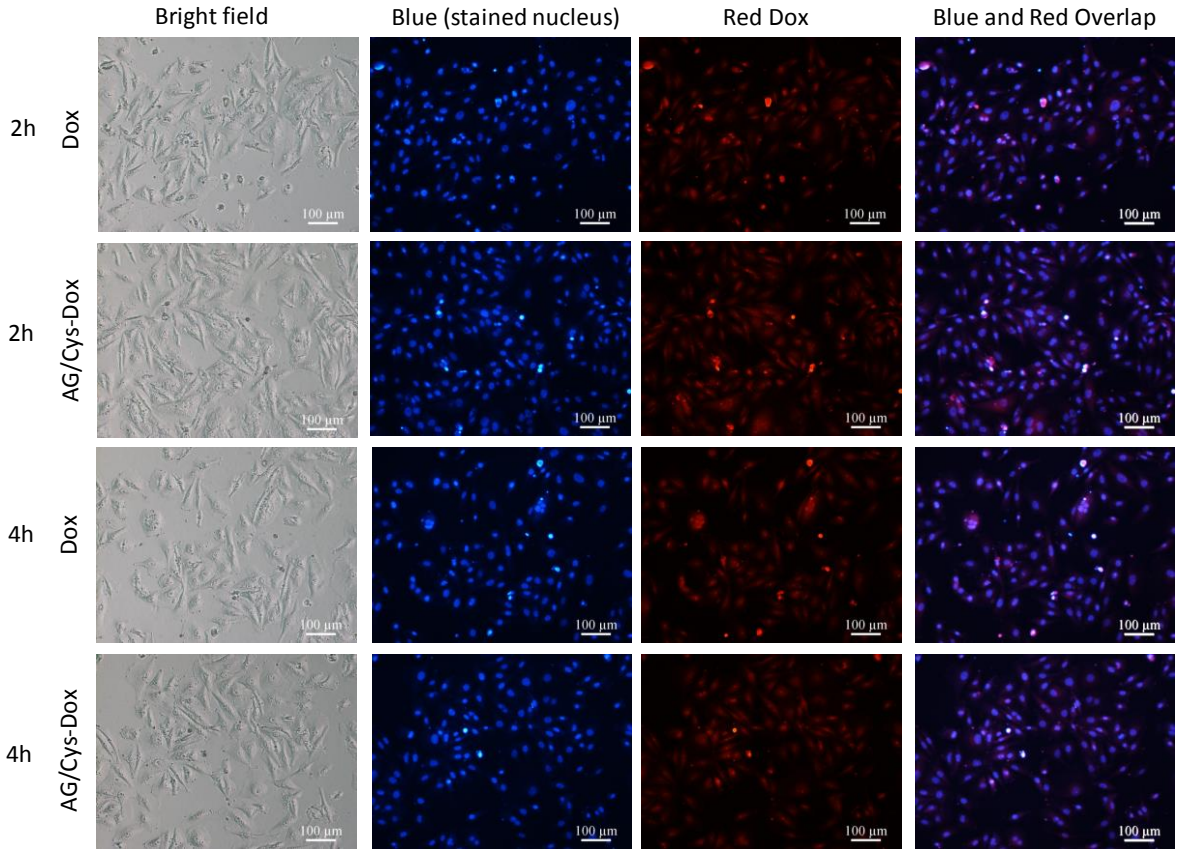

Figure 10. Bright field and fluorescence microscope images of CAL-72 cells after 2 and 4 h culture with free Dox (0.5 μM) and AG/Cys-Dox with an equivalent amount of Dox (0.5 μM). The cell nucleus (blue) is stained with DAPI; Dox emits a red fluorescence signal.

After 48 h in culture, the existence of cell death associated with a high Dox uptake is clearly evident in the assays performed with the AG/Cys-Dox nanogels and for a Dox concentration of 1.5 μM (Figure 11). The improved intracellular delivery of Dox obtained using the nanogels, combined with the accelerated release of Dox in response to the reductive intracellular environment, and a facilitated disruption of the endolysomal vesicles through nanogels action, make the nanogels powerful systems to be used as carriers for positively charged anticancer drugs.

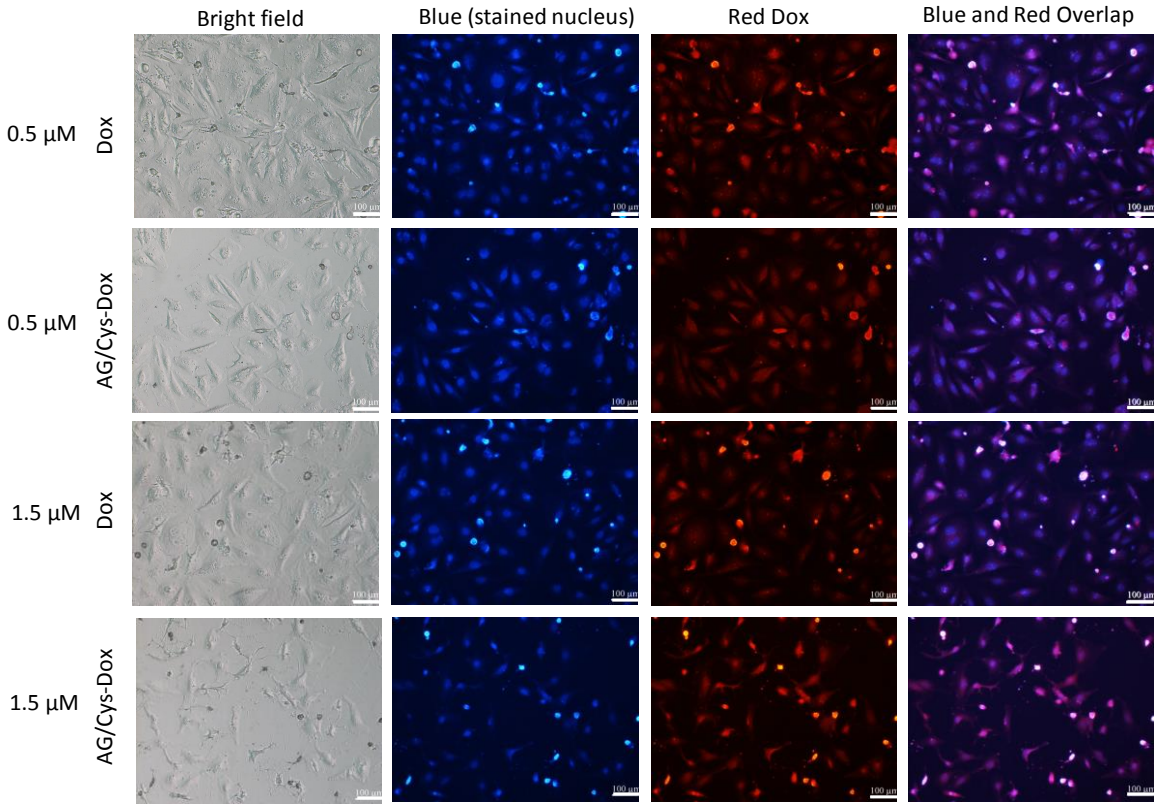

Figure 11. Bright field and fluorescence microscope images of CAL-72 cells after 48 h culture with free Dox (0.5 and 1.5 µM) and AG/Cys-Dox containing an equivalent Dox concentration (0.5 and 1.5 µM). The cell nucleus (blue) is stained with DAPI; Dox emits a red fluorescence signal (The scale bar represents 100 µm).

Conclusions

We developed an easy approach to prepare redox-responsive nanogels to encapsulate Dox. The formed AG/Cys nanogels presented a high drug loading capacity and displayed a redox-controlled drug release sensitivity, which is triggered by conditions mimicking the reducible intracellular environment. The nanogels displayed an excellent cytocompatibility and could be effectively endocytosed by CAL-72 cells with enhanced intracellular Dox accumulation. Also, we believe that the exchange of Dox by protons in the nanogels inside the endolysosomal compartments may help their rupture and the release of Dox into the cytoplasm. In summary, the use of the developed nanogels as vehicles for Dox delivery resulted in an improved *in vitro* anticancer efficacy which might make them promising nanomaterials for the efficient intracellular delivery of anticancer drugs with less side effects *in vivo*.

References

1. Ta HT, Dass CR, Larson I, Choong PF, Dunstan DE. A chitosan-dipotassium orthophosphate hydrogel for the delivery of Doxorubicin in the treatment of osteosarcoma. Biomaterials. 2009;30:3605-3613.

2. Maeng JH, Lee DH, Jung KH, Bae YH, Park IS, Jeong S*, et al.* Multifunctional doxorubicin loaded superparamagnetic iron oxide nanoparticles for chemotherapy and magnetic resonance imaging in liver cancer. Biomaterials. 2010;31:4995-5006.

3. Zhang C, Wang W, Liu T, Wu Y, Guo H, Wang P*, et al.* Doxorubicin-loaded glycyrrhetinic acid-modified alginate nanoparticles for liver tumor chemotherapy. Biomaterials. 2012;33:2187-2196.

4. Weng KC, Noble CO, Papahadjopoulos-Sternberg B, Chen FF, Drummond DC, Kirpotin DB*, et al.* Targeted Tumor Cell Internalization and Imaging of Multifunctional Quantum Dot-Conjugated Immunoliposomes in Vitro and in Vivo. Nano Lett 2008;8:2551-2857.

5. Feridooni T, Hotchkiss A, Remley-Carr S, Saga Y, Pasumarthi KB. Cardiomyocyte specific ablation of p53 is not sufficient to block doxorubicin induced cardiac fibrosis and associated cytoskeletal changes. PLoS One. 2011;6:e22801.

6. Mahoney BP, Raghunand N, Baggett B, Gillies RJ. Tumor acidity, ion trapping and chemotherapeutics. Biochem Pharmacol. 2003;66:1207-1218.

7. Wojtkowiak JW, Verduzco D, Schramm KJ, Gillies RJ. Drug resistance and cellular adaptation to tumor acidic pH microenvironment. Mol Pharmaceutics. 2011;8:2032-2038.

8. Raghunand N, Gillies RJ. pH and drug resistance in tumors. Drug Resist Updat. 2000;3:39-47.

9. Bao L, Haque A, Jackson K, Hazari S, Moroz K, Jetly R*, et al.* Increased expression of P-glycoprotein is associated with doxorubicin chemoresistance in the metastatic 4T1 breast cancer model. Am J Pathol. 2011;178:838-852.

10. Wang S, Konorev EA, Kotamraju S, Joseph J, Kalivendi S, Kalyanaraman B. Doxorubicin induces apoptosis in normal and tumor cells via distinctly different mechanisms. intermediacy of H2O2- and p53-dependent pathways. J Biol Chem. 2004;279:25535-25543.

11. Gao F, Li L, Liu T, Hao N, Liu H, Tan L*, et al.* Doxorubicin loaded silica nanorattles actively seek tumors with improved anti-tumor effects. Nanoscale. 2012;4:3365-3372.

12. Working PK, Newman MS, Sullivan T, Yarrington J. Reduction of Cardiotoxicity of Doxorubicin in Rabbits and Dogs by Encapsulation in Long-Circulating, Pegylated Liposomes. J Pharmacol Exp Ther. 1999;289:1128–1133.

13. Erttmann R, Erb N, Steinhoff A, Landbeck G. Pharmacokinetics of Doxorubicin in Man - Dose and Schedule Dependence. J Cancer Res Clin. 1988;114:509-513.

14. Kaminskas LM, McLeod VM, Kelly BD, Sberna G, Boyd BJ, Williamson M*, et al.* A comparison of changes to doxorubicin pharmacokinetics, antitumor activity, and toxicity mediated by PEGylated dendrimer and PEGylated liposome drug delivery systems. Nanomed-Nanotechnol. 2012;8:103-111.

15. Vrignaud S, Benoit JP, Saulnier P. Strategies for the nanoencapsulation of hydrophilic molecules in polymer-based nanoparticles. Biomaterials. 2011;32:8593-8604.

16. Luo SL, Zhang EL, Su YP, Cheng TM, Shi CM. A review of NIR dyes in cancer targeting and imaging. Biomaterials. 2011;32:7127-7138.

17. Raemdonck K, Braeckmans K, Demeester J, De Smedt SC. Merging the best of both worlds: hybrid lipid-enveloped matrix nanocomposites in drug delivery. Chem Soc Rev. 2014;43:444-472.

18. Prados J, Melguizo C, Ortiz R, Velez C, Alvarez PJ, Arias JL*, et al.* Doxorubicin-Loaded Nanoparticles: New Advances in Breast Cancer Therapy. Anticancer Agent Med Chem. 2012;12:1058-1070.

19. Rapoport N. Physical stimuli-responsive polymeric micelles for anti-cancer drug delivery. Prog Polym Sci. 2007;32:962-990.

20. Zhang CY, Yang YQ, Huang TX, Zhao B, Guo XD, Wang JF*, et al.* Self-assembled pH-responsive MPEG-b-(PLA-co-PAE) block copolymer micelles for anticancer drug delivery. Biomaterials. 2012;33:6273-6283.

21. Jiang XL, Li LH, Liu J, Hennink WE, Zhuo RX. Facile Fabrication of Thermo-Responsive and Reduction-Sensitive Polymeric Micelles for Anticancer Drug Delivery. Macromol Biosci. 2012;12:703-711.

22. MacEwan SR, Callahan DJ, Chilkoti A. Stimulus-responsive macromolecules and nanoparticles for cancer drug delivery. Nanomedicine. 2010;5:793-806.

23. Cheng R, Feng F, Meng F, Deng C, Feijen J, Zhong Z. Glutathione-responsive nano-vehicles as a promising platform for targeted intracellular drug and gene delivery. J Control Release. 2011;152:2-12.

24. Russo A, DeGraff W, Friedman N. Selective Modulation of Glutathione Levels in Human Normal *versus* Tumor Cells and Subsequent Differential Response to Chemotherapy Drugs. Cancer Res. 1986;46:2845-2848.

25. De Cock LJ, De Koker S, De Geest BG, Grooten J, Vervaet C, Remon JP*, et al.* Polymeric multilayer capsules in drug delivery. Angew Chem Int Edit. 2010;49:6954-6973.

26. Grull H, Langereis S. Hyperthermia-triggered drug delivery from temperature-sensitive liposomes using MRI-guided high intensity focused ultrasound. J Control Release. 2012;161:317-327.

27. Kazarov S, Kaholek M, Kudasheva D, Teraoka I, Cowman MK, Levon K. Poly(N-isopropylacrylamide-co-1-vinylimidazole) Hydrogel Nanoparticles Prepared and Hydrophobically Modified in Liposome Reactores: Atomic Force Microscopy and Dynamic Light Scattering Study. Langmuir. 2003;19:8086-8093.

28. Endres TK, Beck-Broichsitter M, Samsonova O, Renette T, Kissel TH. Self-assembled biodegradable amphiphilic PEG-PCL-lPEI triblock copolymers at the borderline between micelles and nanoparticles designed for drug and gene delivery. Biomaterials. 2011;32:7721-7731.

29. Medina SH, Tekumalla V, Chevliakov MV, Shewach DS, Ensminger WD, El-Sayed ME. N-acetylgalactosamine-functionalized dendrimers as hepatic cancer cell-targeted carriers. Biomaterials. 2011;32:4118-4129.

30. Shan YB, Luo T, Peng C, Sheng RL, Cao AM, Cao XY*, et al.* Gene delivery using dendrimer-entrapped gold nanoparticles as nonviral vectors. Biomaterials. 2012;33:3025-3035.

31. Luo Y, Ling Y, Guo W, Pang J, Liu W, Fang Y*, et al.* Docetaxel loaded oleic acid-coated hydroxyapatite nanoparticles enhance the docetaxel-induced apoptosis through activation of caspase-2 in androgen independent prostate cancer cells. J Control Release. 2010;147:278-288.

32. Feazell RP, Nakayama-Ratchford N, Dai H, Lippard SJ. Soluble single-walled carbon nanotubes as longboat delivery systems for Platinum(IV) anticancer drug design. J Am Chem Soc. 2007;129:8438-8439.

33. Prakash S, Malhotra M, Shao W, Tomaro-Duchesneau C, Abbasi S. Polymeric nanohybrids and functionalized carbon nanotubes as drug delivery carriers for cancer therapy. Adv Drug Deliver Rev. 2011;63:1340-1351.

34. Xiao C, Chen S, Zhang L, Zhou S, Wu W. One-pot synthesis of responsive catalytic Au@PVP hybrid nanogels. Chem Commun. 2012;48:11751-11753.

35. Kabanov AV, Vinogradov SV. Nanogels as Pharmaceutical Carriers: Finite Networks of Infinite Capabilities. Angew Chem Int Edit. 2009;48:5418-5429.

36. Li Y, Rodrigues J, Tomás H. Injectable and biodegradable hydrogels: gelation, biodegradation and biomedical applications. Chem Soc Rev. 2012;41:2193-2221.

37. Li Y, Maciel D, Tomás H, Rodrigues J, Ma H, Shi XY. pH sensitive Laponite/alginate hybrid hydrogels: swelling behaviour and release mechanism. Soft Matter. 2011;7:6231-6238.

38. Khdair A, Handa H, Mao G, Panyam J. Nanoparticle-mediated combination chemotherapy and photodynamic therapy overcomes tumor drug resistance *in vitro*. 2009;71:214-222.

39. Khdair A, Chen D, Patil Y, Ma L, Dou QP, Shekhar MP*, et al.* Nanoparticle-mediated combination chemotherapy and photodynamic therapy overcomes tumor drug resistance. J Control Release. 2010;141:137-144.

40. Lee KY, Bouhadir KH, Mooney DJ. Controlled degradation of hydrogels using multi-functional cross-linking molecules. Biomaterials. 2004;25:2461-2466.

41. Chang D, Lei J, Cui HR, Lu N, Sun YJ, Zhang XH*, et al.* Disulfide cross-linked nanospheres from sodium alginate derivative for inflammatory bowel disease: Preparation, characterization, and in vitro drug release behavior. Carbohyd Polym. 2012;88:663-669.

42. Vieira EFS, Cestari AR, Airoldi C, Loh W. Polysaccharide-Based Hydrogels: Preparation, Characterization and Drug Intetaction Behaviour. Biomacromolecules. 2008;9:1195-1199.

43. Clegg RS, Hutchison JE. Hydrogen-Bonding, Self-Assembled Monolayers: Ordered Molecular Films for Study of Through-Peptide Electron Transfer. Langmuir. 1996;12:5239-5243.

44. Kim S-H, Han S-K, Lee S-M, Im J-H, Kim J-H, Koh K-N*, et al.* Preparation and spectroscopic characterization of a self-assembled monolayer of squarylium dye on gold. Dyes Pigments. 2000;45:23-28.

45. Zhao Y, Gao S, Zhao S, Li Y, Cheng L, Li J*, et al.* Synthesis and characterization of disulfide-crosslinked alginate hydrogel scaffolds. Mat Sci Eng C-Mater. 2012;32:2153-2162.

46. Nagasoe Y, Ichiyanagi N, Okabayashi H, Nave S, Eastoe J, O'Connor CJ. Raman and IR spectroscopic studies of the interaction between counterion and polar group in self-assembled systems of AOT-homologous "sodium dialkyl sulfosuccinates". Phys Chem Chem Phys. 1999;1:4395-4407.

47. Gao W, Chan JM, Farokhzad OC. pH-Responsive Nanoparticles for Drug Delivery. Mol Pharmaceutics. 2010;7:1913-1920.

48. Ford J, Khoo SH, Back DJ. The intracellular pharmacology of antiretroviral protease inhibitors. J Antimicrob Chemother. 2004;54:982-990.

CHAPTER III. Dendrimer-Assisted Formation of Fluorescent Nanogels for Drug Delivery and Intracellular Imaging

***This Chapter is based on the following publication:**

Gonçalves M, Maciel D, Capelo D, Xiao S, Sun W, Shi X, Rodrigues J, Tomás H, Li Y. Dendrimer-assisted formation of fluorescent nanogels for drug delivery and intracellular imaging. Biomacromolecules. 2014;15:492-499. (Gonçalves M and Maciel D equally contributed to this work). (Published)

Abstract

Although, in general, nanogels present a good biocompatibility and are able to mimic biological tissues, their instability and uncontrollable release properties still limit their biomedical applications. In this study, a simple approach was used to develop dual-crosslinked dendrimer/alginate nanogels (AG/G5), using $CaCl_2$ as crosslinker and amine-terminated generation 5 dendrimer (G5) as a co-crosslinker, through an emulsion method. *Via* their strong electrostatic interactions with anionic AG, together with crosslinker Ca^{2+}, G5 dendrimers can be used to mediate the formation of more compact structural nanogels with smaller size (433±17 nm) than that (873±116 nm) of the Ca^{2+}-crosslinked AG nanogels in the absence of G5. Under physiological (pH 7.4) and acidic (pH 5.5) conditions, the size of Ca^{2+}-crosslinked AG nanogels gradually decrease probably because of their degradation, while dual-crosslinked AG/G5 nanogels maintain a relatively more stable structure. Furthermore, the AG/G5 nanogels effectively encapsulate the anticancer drug doxorubicin (Dox) with a loading capacity of 3 folds higher than that of AG nanogels. The AG/G5 nanogels were able to release Dox in a sustained way, avoiding the burst release observed for AG nanogels. *In vitro* studies show that the AG/G5-Dox nanogels were effectively taken up by CAL-72 cells (a human osteosarcoma cell line) and maintain the anticancer cytotoxicity levels of free Dox. Interestingly, G5 labeled with a fluorescent marker can be integrated into the nanogels and be used to track them inside the cells by fluorescence microscopy. These findings demonstrate that AG/G5 nanogels may serve as a general platform for therapeutic delivery and/or cell imaging.

Keywords: Fluorescent nanogels; alginate; dendrimer; bioimaging; drug delivery

Introduction

The clinical outcomes of many anticancer drugs, like doxorubicin (Dox), are still not acceptable because of the phenomenon of drug resistance[1]. To achieve a desirable therapeutic efficacy, a large dosage or increased number of injections is often used, which may lead to adverse side effects on normal tissues[2, 3]. However, the use of an appropriate drug nanocarrier can be an adequate tool to overcome this problem[4]. Furthermore, the integration of imaging agents with chemotherapeutics into nanocarriers for simultaneous intracellular tracking and therapy can provide an improved approach in the treatment and study of cancer[5]. In fact, fluorescent molecules can be used to locate materials inside cells and, for that, organic fluorophores and fluorescent proteins are the most widely used[6]. Ideal fluorescent molecules present a few requests such as lasting high brightness, sufficient water dispersibility, good biocompatibility and facility of bioconjugation[6]. Yet, to get nanocarriers with good biocompatibility, sufficient stability and long circulation time is still a challenge for *in vivo* medical applications[6-13].

Nanogels are nanoscale three-dimensional hydrophilic polymer networks that swell in water[14]. The nanogels have Hamaker constants similar to those of water and, so, the driving forces for their aggregation in biological fluids are low[13]. Compared to other nanocarriers, nanogels have good biocompatibility, high aqueous dispersibility and a well-defined structure[15, 16]. Due to these advantages, they are ideal systems to load biomarkers and/or drugs through appropriate physical or chemical conjugation[17]. Moreover, nanogels have been proven to be internalized by cells more efficiently than conventional carriers such as liposomes which are less stable when compared with nanogels[18]. It was also reported that, as drug carriers, nanogels can significantly improve the bioavailability and *in vivo* safety of drugs[19].

As a kind of natural polymer, alginate (AG), a polysaccharide found in nature, is considered to be safe by the U.S. Food and Drug Administration, and has been widely used in a variety of biomedical applications[20]. An emulsion technique has been frequently used to prepare biodegradable AG nanogels for Dox delivery using $CaCl_2$ as a crosslinker[21-23]. However, pure Ca^{2+}-crosslinked AG nanogels are not stable which is probably caused by the rapid exchange of Ca^{2+} with other cations present in the phosphate buffer saline (PBS) solution[22, 24]. Such instability may result in a burst drug release profile, and thus cause reduced therapeutic efficacy and higher side effects to normal organs in the human body[21].

Poly(amidoamine) (PAMAM) dendrimers are macromolecules that have a hydrophobic core and a hydrophilic periphery and can act as effective nanocarriers for delivery of various drugs[25-28]. These dendrimers can be functionalized with other molecules, including targeting ligands, imaging dyes and drugs, making them an excellent platform for specific targeting, gene transfection, imaging and disease treatment[28, 29]. However, PAMAM dendrimers can result in high cytotoxicity mainly due to the damage caused by their high positively charged surface on the negatively charged cell membrane[30]. Considering their strong electrostatic interactions with anionic AG, it is hypothesized that cationic amine-terminated PAMAM dendrimers might be used, together with $CaCl_2$, to develop AG nanogels with more controllable properties. On one hand, the dendrimers with a highly cationic charged surface are expected to enhance the stability of Ca^{2+}-crosslinked AG nanogels through their strong electrostatic interactions[6]. On the other hand, the shielding of AG on the surface of the dendrimers may improve the biocompatibility of the dendrimers. In addition, the use of multivalent dendrimers may endow AG nanogels with multifunctionality[8].

In the present study, a new type of nanogels was developed by incorporating generation 5 amine-terminated PAMAM dendrimers (G5) and Dox into AG nanogels by using an emulsion method, where both $CaCl_2$ and dendrimers acted as crosslinkers (). The stability, drug release behavior and anticancer cytotoxicity of the formed nanogels were investigated. Our results indicate that the dendrimers can be used to mediate the nanogels formation with better stability and drug release sustainability than the simple Ca^{2+}-crosslinked AG nanogels. The Dox-loaded AG/G5 nanogels kept the anticancer bioactivity of Dox uncompromised. Furthermore, the amine-terminated G5 was further conjugated with fluorescein isothiocyanate (FI) to form a macromolecular imaging agent (G5-FI) that, once incorporated in the nanogels, allowed their visualization inside cells.

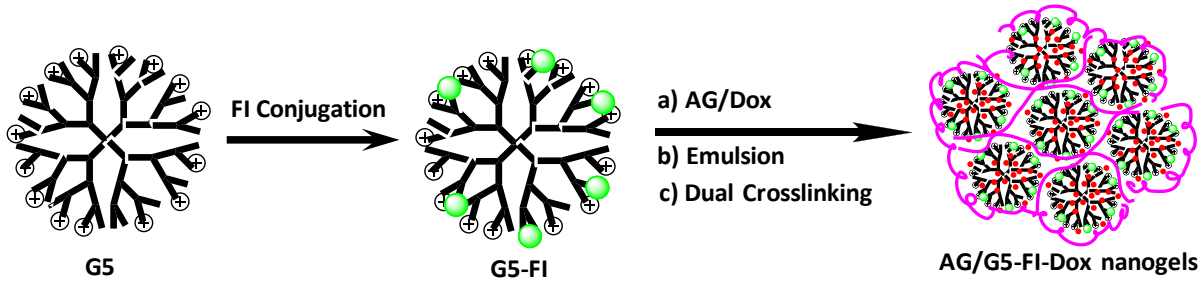

Figure 12. Schematic overview of the nanogels conjugated with FI, with Dox encapsulation and the dual-crosslink.

Materials and Methods

Materials

Ethylenediamine core amine-terminated G5 PAMAM dendrimers (G5) with a polydispersity index less than 1.08 were purchased from Dendritech (Midland, MI), USA. Fluorescein Isothiocyanate (FI) was obtained from Sigma, USA. Alginate acid sodium salt (AG) (from brown Algae, M_w from 12 to 58 kDa, cell culture tested) was bought from Sigma, USA. Doxorubicin hydrochloride (Dox) was obtained from Zibo Ocean International Trade Co, Ltd., China. Dioctyl sodium sulfosuccinate (AOT) was obtained from Sigma-Aldrich, USA. Polyvinyl alcohol (PVA, M_w 72 kDa) was purchased from Merck, Germany. Dulbecco's phosphate buffer saline (PBS) solution (without Ca^{2+} and Mg^{2+}) was purchased from Panreac, Spain. Regenerated cellulose dialysis membrane (molecular weight cutoff, MWCO 14 kDa) was acquired from Spectra/Por, USA. 4',6-diamidino-2-phenyindole dilactate (DAPI) was bought from Sigma, USA. Glutaraldehyde was obtained from Sigma, USA. All other chemicals were obtained from Aldrich and used as received.

Synthesis of FI-Functionalized Dendrimers (G5-FI)

G5 was conjugated with FI moieties, as previously reported by our team[29]. Briefly, a solution of FI (8.2 mg, 0.02106 mmol) in DMSO (5 mL) was dropped in a solution of G5 (100 mg, 0.00347 mmol) in ultrapure water (20 mL) under 400 rpm stirring at room temperature. The reaction proceeded for 24 h. The solution was dialyzed against PBS buffer (3 times, 1 L) and water (3 times, 4 L) for 3 days through a 14 kDa MWCO membrane, and lyophilized to give the orange product G5-FI. The G5 conjugates were characterized by ^{1}H NMR. The number of FI moieties conjugated onto each G5 dendrimer (6.1) was estimated using the integrals of the ^{1}H NMR signals associated with the dendrimers and the FI moieties[29].

Preparation and Physical Characterization of AG/G5-Dox Nanogels

One gram of AG/G5-Dox (1/0.5/x wt%, x = 0 or 0.2) or AG/G5-FI (1/0.5 wt %) aqueous solution in the absence or presence of 0.1 mL of 1 M sodium hydroxide (NaOH) solution, respectively, was dropped into 2 mL of 2.5 wt % AOT solution in dichloromethane

(DCM) under stirring (400 rpm) at room temperature. The selected Dox concentration was based on the results obtained in one of our previous reports[4]. The mixture was stirred under 400 rpm for 5 min, and then was dropped into 15 g of 2 wt % PVA aqueous solution, followed by stirring at 400 rpm for 30 min. Afterwards, 5 mL of 60 wt % of calcium chloride ($CaCl_2$) aqueous solution was dropped into the above solution, and then stayed overnight under stirring at 400 rpm for evaporation of DCM. The obtained mixture was centrifuged (12 000 rpm for 5 min) and washed with distilled water (25 mL x 3 times). The precipitate was lyophilized for 3 days to get AG/G5, AG/G5-Dox and AG/G5-FI nanogels. The concentration of Dox was determined in the supernatants by spectrophotometry at 490 nm using an ultraviolet-visible (UV-Vis) spectrometer (Lambda 2, Perkin-Elmer) for indirect calculation of Dox encapsulation efficiency. The AG nanogels with or without Dox, in the absence of PAMAM dendrimers, were also prepared in a similar way as above, and named as AG and AG-Dox nanogels, respectively.

The particle size and zeta potential of the AG-Dox and AG/G5-Dox nanogels were measured using a Zetasizer Nano ZS (Malvern Instruments) equipment. The nanogels were dispersed in PBS under sonication for 15 min before measurements. The morphology of the AG-Dox and AG/G5-Dox nanogels was examined by scanning electron microscopy (SEM, JSM-5600LV, JEOL Ltd., Japan) with an operating voltage of 10 kV. Before measurement, the samples were dispersed in ultrapure water under sonication for 10 min. The aqueous suspensions of the samples were dropped onto an aluminum foil, air-dried, an Au-sputtered coated before analysis.

In vitro drug release studies

In triplicate, 1 mg of Dox-loaded nanogels was dissolved in 2 mL PBS at the pH values of 7.4 and 5.5 and kept at 37 ºC. At each predetermined time interval, the solution was centrifuged at 12 000 rpm for 2 min at room temperature. The supernatant was taken out and Dox concentration was determined spectrophotometrically at 490 nm at different intervals using an ultraviolet-visible (UV-Vis) spectrometer.

The cumulative release (C_r) of Dox against time was obtained according to the equation:

$$C_r = 100 * Abs_t / Abs_{tot} \quad (1)$$

Where Abs_t and Abs_{tot} are the cumulative amount of drug released at time t and the total drug contained in the nanogels used for drug release, respectively.

Biological Assays

CAL-72 cells (a human osteosarcoma cell line) and NIH 3T3 fibroblasts (used as a model of normal cells) were cultured in Dulbecco's Modified Eagle Medium (D-MEM) containing 10% (v/v) fetal bovine serum (FBS, Gibco) and 1% (v/v) of an antibiotic-antimycotic 100x solution (AA, Gibco, with penicillin, streptomycin, and amphotericin B). For CAL-72 cells the medium was supplemented with 1% (v/v) of L-glutamine 100x solution (Gibco) and 1% (v/v) of insulin-transferin-selenium 100x solution (ITS, Gibco). Both cell lines were grown at 37 ºC at a humidified atmosphere with 5% carbon dioxide. Afterwards, the cells were harvested at 70-80% confluence, using trypsin-EDTA solution for the enzymatic detachment of the cells from the plastic substrate.

For the cytotoxicity experiments, CAL-72 cells and NIH 3T3 fibroblasts were first plated in 48-well plates at a seeding density of 12 x 10^3 cells per well. After one day, free Dox, AG-Dox and AG/G5-Dox nanogel solutions (with equivalent Dox concentrations), prepared in PBS buffer, were added to the cell culture media and then incubated for 48 h, at 37 ºC, before the resazurin reduction assay. Solutions of PBS, G5, AG and AG/G5 nanogels in PBS buffer were used as controls. Solutions of G5-FI and AG/G5-FI nanogels with equivalent mass concentration were employed for the cytotoxicity and cell imaging study.

The cell viability was quantified by the measurement of the metabolic activity of the cells in culture through the resazurin reduction assay[31, 32]. Briefly, after the 48 h incubation time, the cell culture medium was replaced with fresh medium containing resazurin at a concentration of 0.1 mg/mL, and kept at 37 ºC for 3 h. Afterwards, aliquots of the cell supernatant were transferred to 96-well opaque plates and the resorufin fluorescence (λ_{ex}=530 nm, λ_{em}=590 nm) was measured using a microplate reader (model Victor^3 1420, Perkin-Elmer). Statistical analyses were performed using the IBM SPSS Statistics 20 software (IBM Inc., Armonk). One-way ANOVA with Tukey Post Hoc test was used to assess the statistical difference between group means.

For the cell uptake study, cells were plated for 24 h before the incubation with the test solutions, to allow cell attachment. In these experiments, solutions of free Dox, AG-Dox and AG/G5-Dox nanogels were used at the same Dox concentration (the final concentrations in the wells were 0.5 μM). Cells were then incubated with the test solutions at 37 ºC for 4 h. Subsequently, the cultures were washed with sterilized PBS buffer, fixed with 3.7% glutaraldehyde and stained with DAPI for 30 min, and visualized using a fluorescence microscope (Nikon Eclipse TE 2000E).

Results and Discussion

Preparation and Physical Characterization of Dox-loaded Nanogels

The nanogels preparation was done according to the emulsion method presented in Figure 13. This method allows the formation of monodispersed nanoparticles which can be tuned by the presence of surfactant(s)[4]. Table 2 shows the size (measured by dynamic light scattering (DLS)) and the zeta potential of the nanogels measured in PBS buffer. The AG nanogels had a size of 873±116 nm and a zeta potential of -75.0±4.5 mV, while AG/G5 nanogels had a size of 433±17 nm and a zeta potential of -49.8±1.2 mV. The decrease in the size and increase in the zeta potential in AG/G5 nanogels indicates that the cationic G5 dendrimers have been successfully integrated into AG nanogels which may have a more compact structure due to the strong electrostatic interactions between the G5 and anionic AG. The size decrease, together with their negatively charged surface, may be beneficial to the improvement of the *in vivo* stability of the AG nanogels, through reducing the possibility of their phagocytosis (large particles with a diameter of 2-3 μm can be taken up by phagocytosis) and negatively charged protein adsorption in plasma[33]. The higher zeta potentials of Dox-loaded nanogels compared to those of Dox free nanogels suggest the effective loading of the cationic Dox drug[4]. The incorporation of G5 into the AG nanogels increased three times their loading capacity (Table 2).

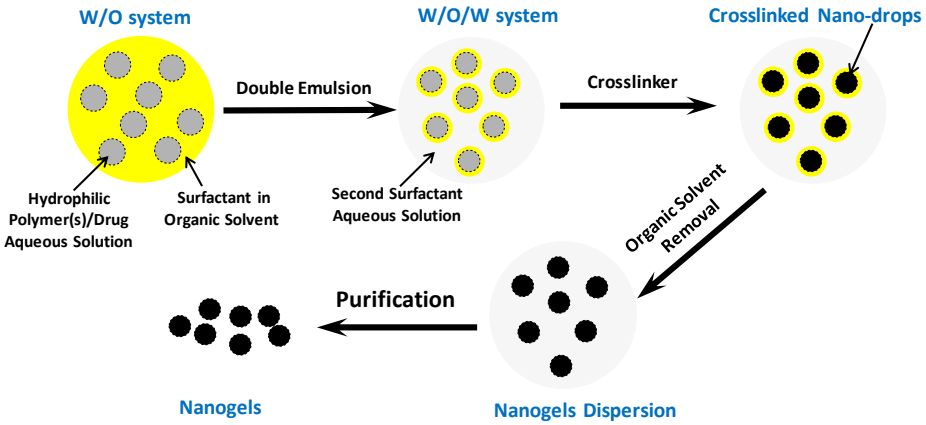

Figure 13. Schematic illustration of the formation of nanogels through a double emulsion method. Usually, an aqueous solution of hydrophilic polymers (precursor) is emulsified in a surfactant organic solvent to form a water-in-oil (W/O) system. The mixture is then re-emulsified in an aqueous solution of a second surfactant to obtain a water-in-oil-in-water (W/O/W) system. The double-emulsified drops undergo physical and/or chemical crosslinking, followed by organic solvent removal and purification (*e.g.*, centrifugation) to obtain nanogels.

Table 2. Characterization of Dox-free and Dox-loaded nanogels[2].

Sample	Size, nm[a]	Zeta Potential, mV	EE, %[b]	LC, %[c]
AG	873±116	-75.0±4.5	-	-
AG-Dox	840±108	-66.7±2.9	31.8±0.9	1.8±0.1
AG/G5	433±17	-49.8±1.2	-	-
AG/G5-Dox	374±6	-39.9±1.9	72.5±0.2	5.6±0.2
AG/G5-FI	462±17	-41.9±3.7	-	-

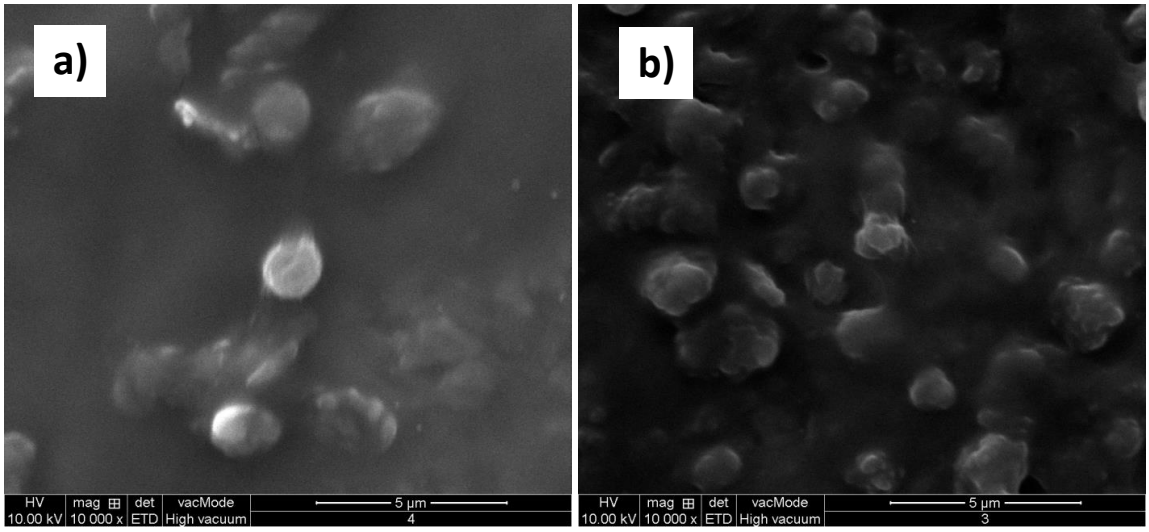

Figure 14. Scanning Electron Microscope (SEM) images of the AG-Dox (a) and AG/G5-Dox (b) nanogels.

The Dox-loaded AG and AG/G5 nanogels were further examined by Scanning Electron Microscopy (SEM). As shown in Figure 14, it is evident that both nanogels are present as dispersed nanoparticles, with larger sizes than those measured by DLS, probably because of the extension of soft nanogels on the surface during their dry process for SEM analysis. Generally, AG/G5-Dox nanogels had a smaller size than those obtained for AG-Dox nanogels, which is in agreement with the results of DLS analysis.

[2] The results are expressed as the mean±standard deviation (n = 3). [a] Size and zeta potential were measured after 2 h incubation in PBS at pH 7.4. [b] Encapsulation efficiency = $100*W_t/W_0$, W_0 and W_t are the total Dox weight used for encapsulation and the weight of encapsulated Dox, respectively. [c] Loading capacity = $100*W_t/W$, W_t and W are the weight of encapsulated Dox and the weight of Dox-loaded nanogels, respectively.

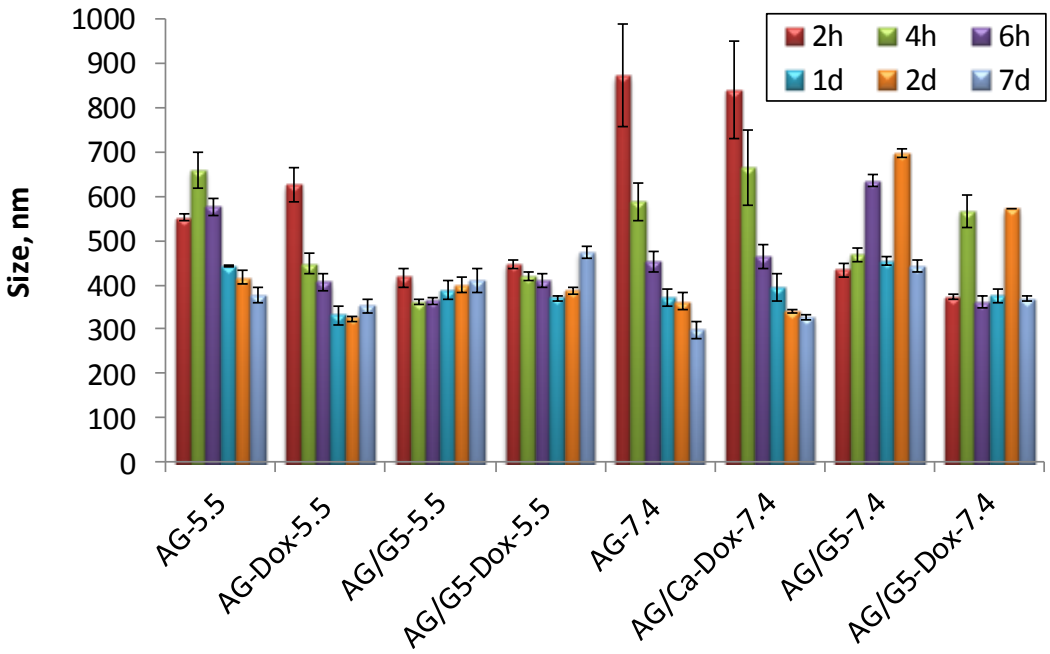

Figure 15. Sizes of AG, AG-Dox, AG/G5 and AG/G5-Dox nanogels in PBS as a function of time at the pH values of 7.4 and 5.5. The results are expressed as the mean ± standard deviation (n = 3).

It is known that the stability of the nanocarriers in the physiological environment is important for their *in vivo* applications[34]. In order to evaluate the stability of the nanogels, their hydrodynamic sizes were analyzed in PBS solution at two different pH values (7.4 and 5.5) (Figure 15). Under physiological conditions (pH 7.4), the sizes of AG nanogels before and after Dox loading gradually decreased with the increase of the incubation time (the experiments were done along 7 days), probably because of the degradation of the nanogels caused by the rapid exchange of Ca^{2+} with the cations in the PBS buffer[22, 24]. Compared to the corresponding AG systems, AG/G5 nanogels in the absence or presence of Dox had less fluctuations in their size during the same period, indicating that the presence of G5 improved the nanogel stability, possibly through the co-crosslinking of AG macromolecules with G5 and Ca^{2+}. The Dox loading seems not to have a significant effect on the size behavior of both AG and AG/G5 nanogels under similar treatments.

Generally, the sizes of the nanogels at pH 7.4 are larger than those of the corresponding ones at pH 5.5, suggesting that the nanogels presented a more condensed structure at pH 5.5. The pK_a of AG is 3.49[35]. PAMAM dendrimers have a pK_a value of 9.2 for their primary amine groups, and a pK_a of 6.7 for their tertiary amine groups[36]. At pH 5.5, AG/G5 also had a more stable structure than AG nanogels, which may be reasonably attributed to the enhanced crosslinking density of the anionic AG in the presence of the cationic G5

dendrimers[37]. As PAMAM dendrimers undergo higher degree of protonation at pH 5.5 than at pH 7.4, a denser crosslinking and a decreased size are expected at pH 5.5. Therefore, the G5 dendrimers enable the formation of a more compact complex with negatively charged AG through electrostatic interactions[36, 38]. Interestingly, even though AG/G5-Dox appeared to have smaller sizes than those of AG/G5 under physiological conditions (pH 7.4), the previous exhibited larger sizes than those after at acidic conditions (pH 5.5), which may be caused by Dox protonation that induces the swelling of the nanogels[39].

In vitro drug release of Dox-loaded nanogels

For anticancer therapeutic applications, the encapsulated Dox should be able to be released into cancer cells to exert its biological activity. However, nanogels with loose and uncontrollable structure may result in a burst release due to the rapid escape of the drug from their interior[24]. In Figure 16, it can be seen that the release kinetics of Dox from AG/G5-Dox was investigated *in vitro*, in PBS solution, at pH values of 7.4 and 5.5, using AG-Dox as a control. At the physiological pH value, a burst release (56.7%) occurred in AG-Dox within 1 h, while only 21.3% of Dox was released from AG/G5-Dox during the same period. The burst release of AG-Dox may be ascribed to the fast disintegration of AG caused by the rapid exchange of Ca^{2+} with cations in the PBS solution[22, 24]. The presence of G5 as a co-crosslinker for AG/G5-Dox resulted in a denser structure and better stability, thus reducing the burst release. It has to be mentioned that G5 dendrimers can also act as a drug carrier for Dox delivery, which may also limit the Dox release rate from the nanogels[8]. After 2 h of incubation, Dox concentration rapidly decreased (from 56.7% at 2 h to 35.8% at day 12, probably due to the degradation of free Dox induced by hydrolysis in PBS solution[40]. As an alternative, AG/G5-Dox nanogels kept a constant level of drug concentration until day 12, which may be attributed to their sustainability in drug release[41].

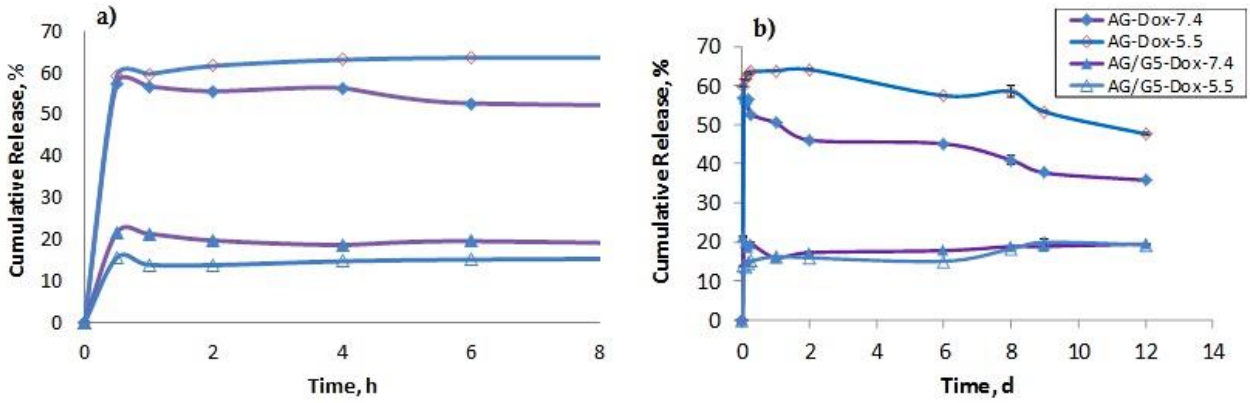

Figure 16. The cumulative release profile of Dox from AG-Dox and AG/G5-Dox nanogels in PBS buffer at the pH values of 7.4 and 5.5. An enlarged graph of the first 8 h (a), and during 12 days (b). The results are expressed as the mean ± standard deviation (n = 3).

With a decrease of the pH value from 7.4 to 5.5, the Dox release rate and release efficiency of the AG-Dox were improved. Probably this happens because Dox diffusion rate increased due to its protonation under acidic conditions and thus higher hydrophilic character. Interestingly, the AG/G5-Dox maintained a sustained release in an acidic environment and kept a high level concentration of Dox during a long period of time (12 days). That is, the presence of G5 endowed the nanogels with a sustainable release ability and good release efficiency at the pH 5.5 (near the pH of the endolysosomal compartments), which may be beneficial in terms of long-term anticancer activity. Inclusive, these results further confirm the role played by dendrimer crosslinking and indicate that the nanogels afford a sustained release of the drug over time.

In vitro cytotoxicity and cellular internalization of Dox-loaded nanogels

To test the biocompatibility of the AG/G5 and the antitumor activity of the AG/G5-Dox, a cell viability assay was carried out using CAL-72 cells, based on the metabolic activity of cells in culture. As can be seen in Figure 17, G5 dendrimers were very toxic for CAL-72 cells at all tested solutions. Comparatively, AG/G5 nanogels exhibited a good biocompatibility (even better than those of the corresponding AG nanogels at higher concentrations). It is known that cationic dendrimers can establish strong interactions with biological membranes, which causes high cytotoxicity by inducing membrane disruption *via* nanohole formation, membrane thinning and erosion[28, 42]. Due to the existence of strong

electrostatic interactions between anionic AG and cationic G5, the anterior can act as a biocompatible coating that shields the cationic surface of G5. In fact, our results show that the zeta potential of AG/G5 nanogels is negative (-49.8±1.2mV, Table 2), indicating the presence of negative surface charges in AG/G5 nanogels[43, 44]. This may be the main reason why AG can improve the biocompatibility of G5 dendrimers.

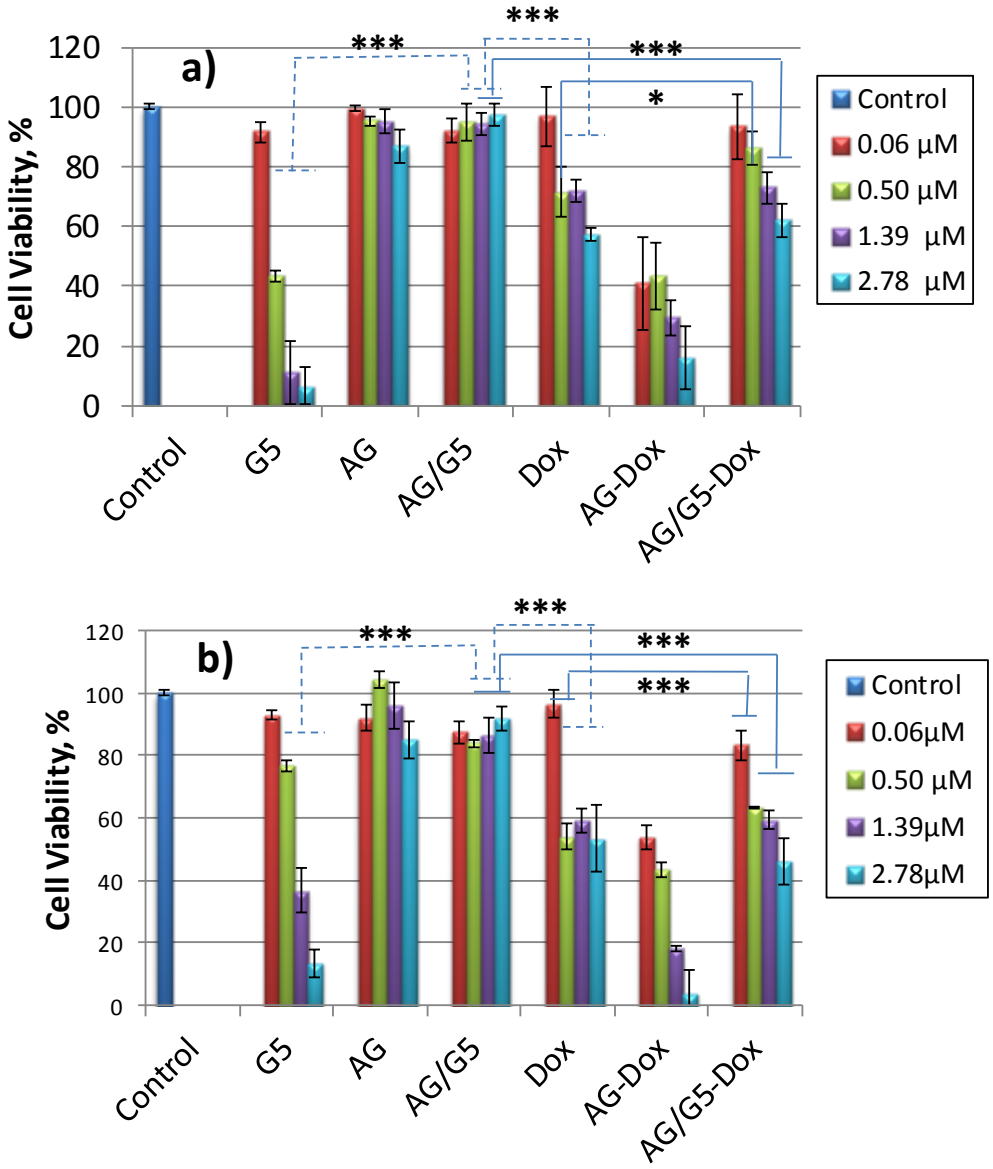

Figure 17. Cytotoxicity of AG/G5-Dox nanogels after 48 h using CAL-72 cells (a) and NIH 3T3 cells (b). AG-Dox, AG/G5-Dox and free Dox had equivalent Dox concentrations. G5, AG/G5 and AG/G5-Dox nanogels had equivalent weight concentrations. Results are reported as the mean ± standard deviation (n = 4). One-way ANOVA with Tukey's Post Hoc test was used to assess the statistical difference between the group means (*$p < 0.05$, ***$p < 0.001$).

More importantly, Dox-loaded AG/G5 were able to inhibit the growth of CAL-72 cells, with inhibition efficiency comparable to that of the free Dox. For example, at a Dox concentration of 2.78 μM, almost 40% of CAL-72 cells died after treatment with both free Dox and AG/G5-Dox samples. Under the same conditions, the Dox-free AG/G5 did not induce any cytotoxicity, showing cell viability (97%) similar to the untreated control cells. Therefore, the anticancer bioactivity is only caused by the loaded drug within the nanogels. It has to be noted that around 20% of released Dox during the cell culture time (48 h) produced a similar *in vitro* anticancer activity to that achieved by free Dox alone (100%). Although AG-Dox had higher cytotoxicity to CAL-72 cells, it was even more toxic to NIH 3T3 cells. This means that, *in vivo*, the use of these materials may result in severe side effects in normal organs. As such, it is believed that the sustainability in Dox release of AG/G5-Dox nanogels, together with their small size (smaller than the size of AG-Dox nanogels), is important for *in vivo* therapeutic applications, specifically to maintain a long-term anticancer bioactivity.

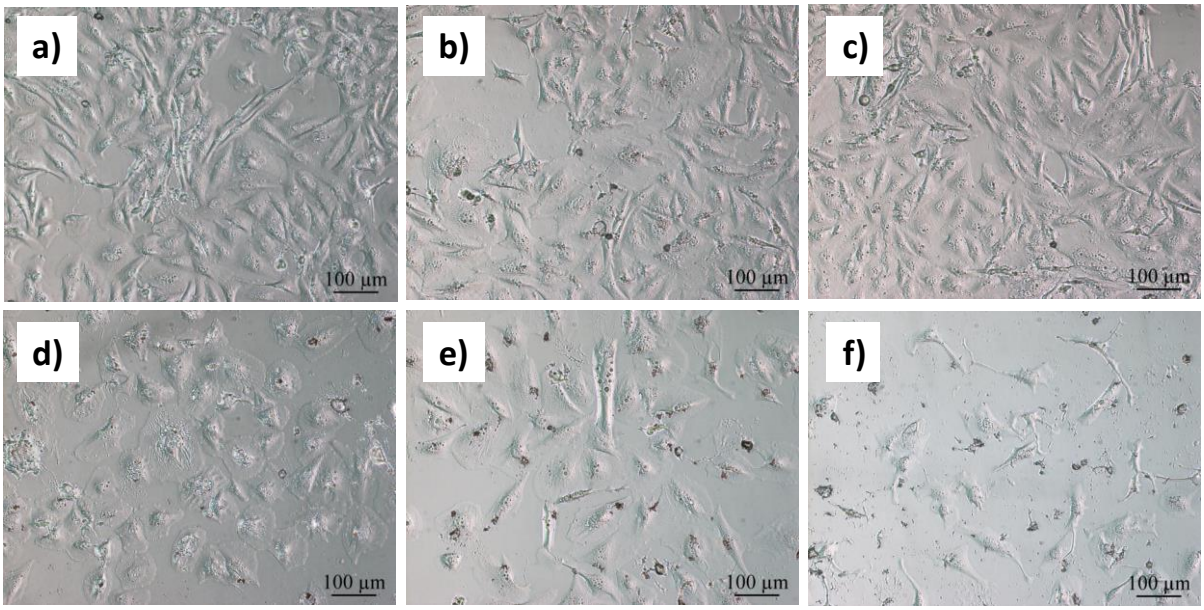

Figure 18. Cell morphology of CAL-72 cells after 48 h in culture with (a) control, (b) AG/G5, (c) AG, and (d) free Dox (2.78 μM), and (e) AG/G5-Dox nanogels and (f) AG-Dox with an equivalent amount of Dox (2.78 μM).

To further confirm the antitumor activity of the Dox-loaded nanogels, the morphology of cells after 48 h incubation with free Dox, AG nanogels and AG/G5 nanogels with and without Dox, were investigated by optical microscopy (Figure 18). Cells treated with PBS (control) and those treated with Dox-free AG and AG/G5 nanogels maintained a healthy

morphology (a fusiform shape and adherence on the cell dish surface). This indicates that both AG and AG/G5 nanogels are quite cytocompatible. At a Dox concentration of 2.78 μM, fusiform (attached cells) and rounded (non-adherent cells or cells in a process of losing the adherence to the surface) cells existed in the samples treated with free Dox and AG/G5-Dox, indicating that they had a similar cytotoxicity. However, at the same Dox concentration, more cells cultured with AG-Dox died, as it can be observed by the existence of less adherent cells and more cell debris. The cell morphology results are in line with the metabolic activity quantitative data, indicating that Dox within the AG/G5-Dox did not weaken the antitumoral activity of free Dox.

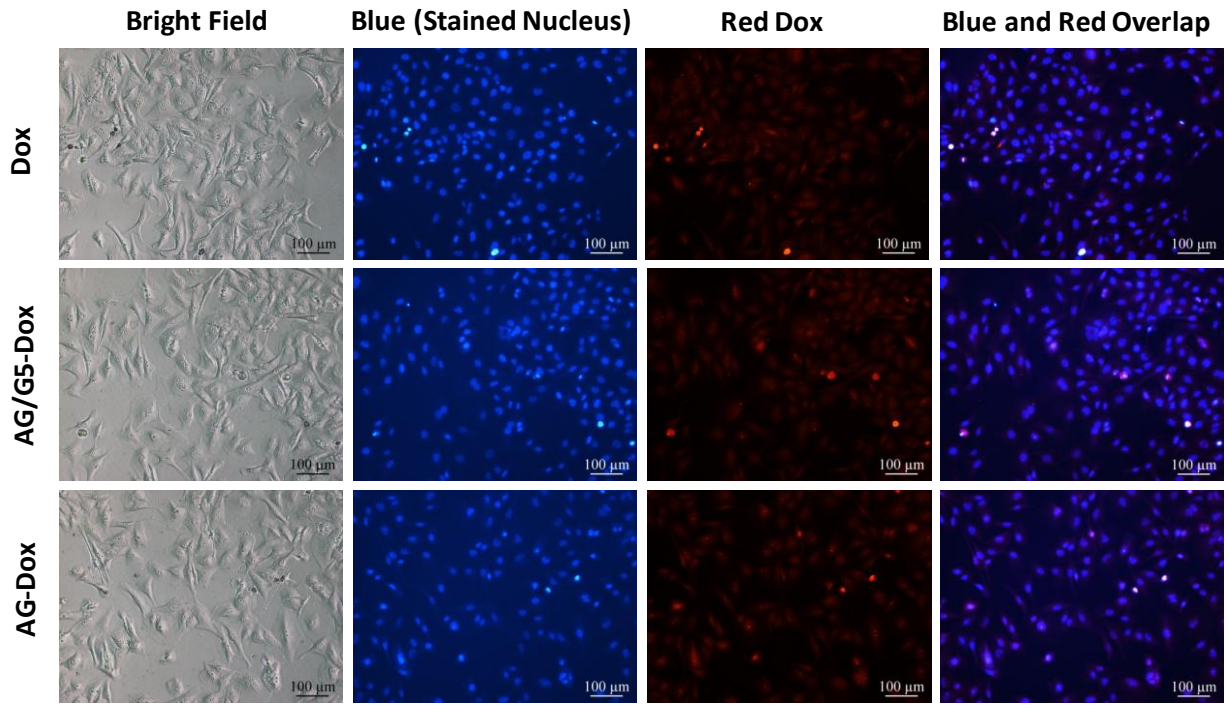

Figure 19. Optical and fluorescence microscope images of CAL-72 cells after 4 h culture with free Dox (0.50 μM), AG/G5-Dox and AG-Dox nanogels with an equivalent amount of Dox (0.50 μM).

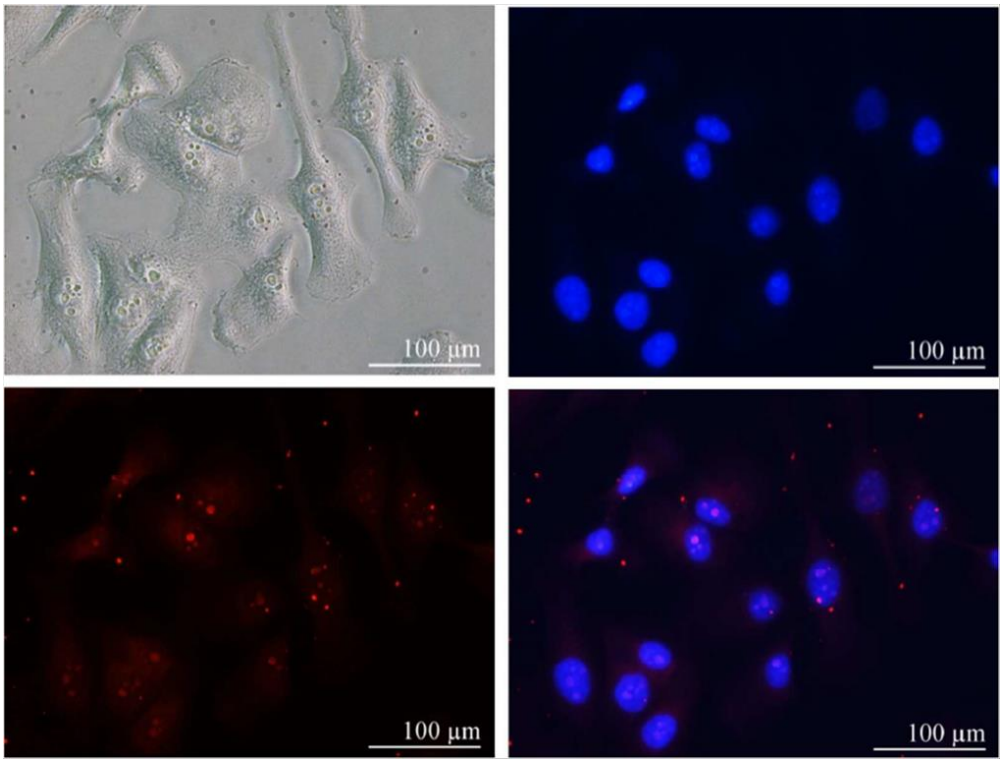

Figure 20. Enlarged optical and fluorescence microscope images of CAL-72 cells after 4 h culture with AG/G5-Dox nanogels with an amount of Dox (0.50 µM). The cell nucleus (blue) is stained with DAPI; Dox emits a red fluorescent signal (300x magnification).

Taking advantage of its fluorescent nature, the extent of Dox internalization in CAL-72 cells was evaluated by fluorescence microscopy, after their exposure to the drug, and AG-Dox and AG/G5-Dox nanogels (Figure 19 and Figure 20). A red fluorescence signal was visualized in cell cytoplasm for all situations under study. Compared to the free Dox, cells cultured in the presence of the Dox-loaded nanogels displayed a stronger red fluorescence, indicating that the presence of nanogels accelerates the Dox uptake process. Considering the ability of AG/G5-Dox nanogels to sustain the drug release, we believe that they can act as Dox shuttles across the cell membrane and facilitate its intracellular release, resulting in a prolonged anticancer activity[45].

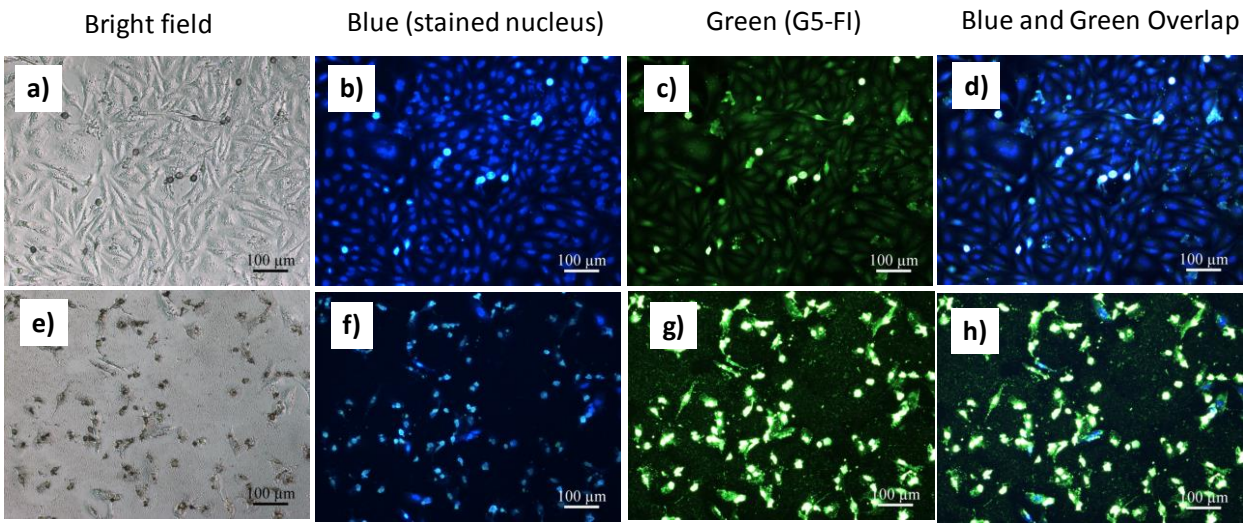

Figure 21. Optical and fluorescence microscopy images of CAL-72 cells after 48 h culture with (a-d) AG/G5-FI nanogels (50 µg/mL), (e-h) G5-FI (50 µg/mL).

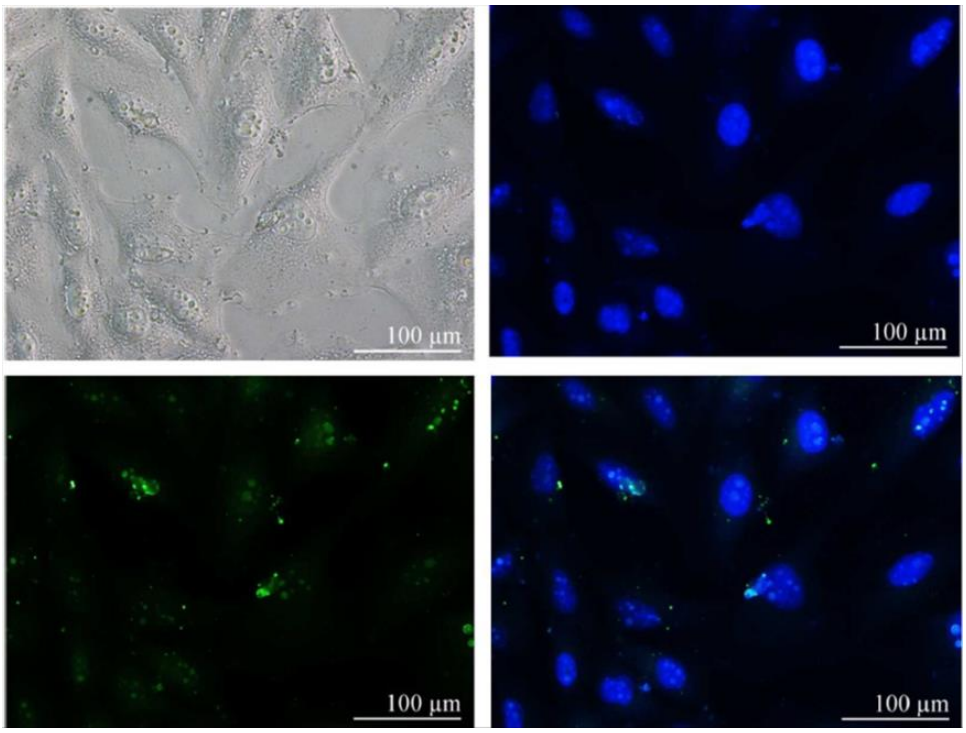

Figure 22. Enlarged optical and fluorescence microscopy images of CAL-72 cells after 48 h culture with AG/G5-FI nanogels (50 µg/mL). The cell nucleus (blue) is stained with DAPI; FI emits a green fluorescent signal (300x magnification).

The efficient uptake of the nanogels by cells is also one of the key factors for achievement of therapeutic efficacy[46]. The inclusion of a fluorescent probe into the nanogels

can provide valuable information concerning the path followed by the drug nanocarrier. Therefore, we synthesized a macromolecular bioimaging marker (G5-FI) by conjugating G5 with a fluorescent molecule, fluorescein isothiocyanate (FI). G5 dendrimer was conjugated with FI, confirmed through NMR analysis (Figure 23). Then using a similar approach, G5-FI was used, instead of G5, for fabrication of AG/G5-FI nanogels (462±17 nm). To check if the nanogels could be internalized and accumulated in cells for bioimaging, CAL-72 cells were incubated with the nanogels for 48 h, respectively. After treatment, cells were fixed and visualized by fluorescence microscopy. As can be seen in Figure 21 and Figure 22, both green (due to FI fluorescence emission) and blue (due to DAPI fluorescence emission) colors were observed in cell cultures after 48 h incubation, which indicated that the nanogels could be effectively taken up by cells, maybe through two popular mechanisms of both phagocytosis and diffusion *via* cell walls, in agreement with the previous report[47].

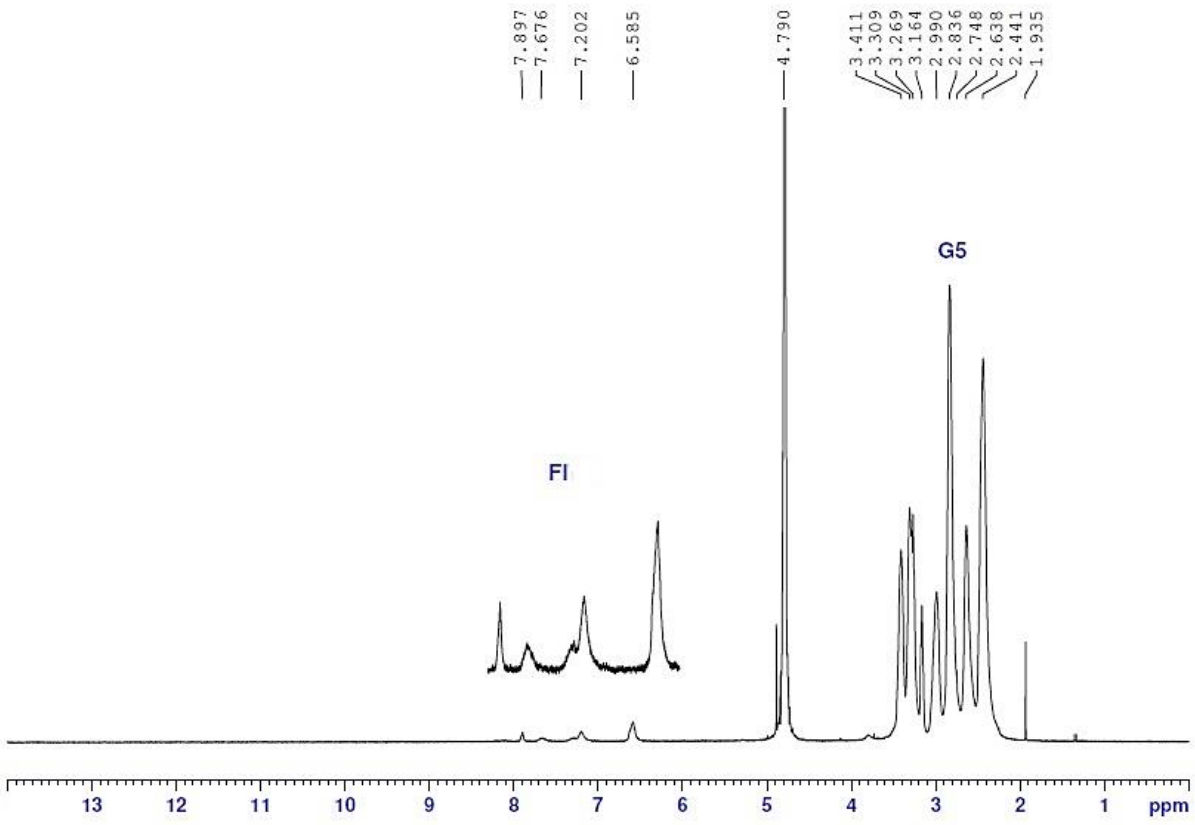

Figure 23. ^{1}H NMR spectrum of G5-FI in D_2O.

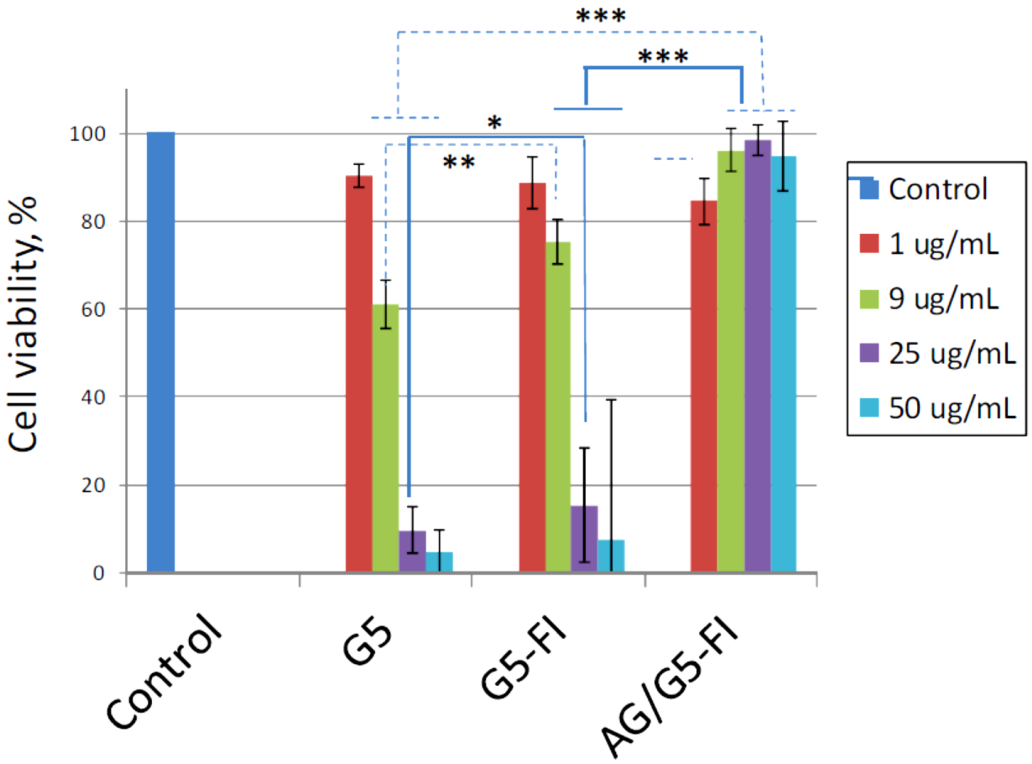

Figure 24. Cytotoxicity of G5, G5-FI and AG/G5-FI nanogels after 48 h incubation with CAL-72 cells. G5, G5-FI, and AG/G5-FI nanogels had equivalent weight concentrations. Results are reported as the mean ± standard deviation (n = 3). One-way ANOVA with Tukey's Post Hoc test was used to assess the statistical difference between the group means (*$p < 0.05$, **$p < 0.01$, ***$p < 0.001$).

Most significantly, after 48 h of incubation the cells treated with AG/G5-FI did not change the cell morphology, suggesting that they have good biocompatibility. Contrarily, G5-FI dendrimers were very toxic, inducing the death of almost all the cells. These results are in agreement with the quantitative data obtained in the corresponding cell viability assays shown in Figure 24. The properties above make us believe that the nanogels can act as a very interesting platform for therapeutic and bioimaging purposes.

Conclusions

We report an elegant approach to construct stable AG/G5 nanogels using both $CaCl_2$ and PAMAM G5 dendrimers as crosslinkers through a double emulsion method. The AG-based nanogels were shown to be stable and biocompatible. In these nanogels, the G5 dendrimers, through their strong electrostatic interactions with anionic AG, are able to assist the formation of nanogels that are more compact than those prepared using only Ca^{2+} cations as a crosslinking agent. The presence of G5 can increase by 3 folds the loading capacity of the anticancer drug Dox in AG nanogels, and maintain an ability to sustain Dox release by avoiding its burst release occurring in AG nanogels. Furthermore, the Dox-loaded AG/G5 nanogels can be effectively taken up by CAL-72 cells (a human osteosarcoma cell line) and intracellular deliver the drug to exert its anticancer cytotoxicity. In addition, G5 dendrimers marked with a fluorescent molecule can be incorporated into the nanogels and allow their tracking by fluorescence microscopy once inside cells. In conclusion, the nanogels exhibit a sustainable delivery of an anticancer drug as well as an intracellular imaging function through fluorescent detection. The presented results demonstrate that AG/G5 nanogels are expected to be a promising platform for therapeutic delivery and/or bioimaging applications.

References

1. Yin Q, Shen J, Zhang Z, Yu H, and Li Y. Reversal of multidrug resistance by stimuli-responsive drug delivery systems for therapy of tumor. Adv Drug Deliv Rev. 2013;64:1699-1715.

2. Wang SW, Konorev EA, Kotamraju S, Joseph J, Kalivendi S, Kalyanaraman B. Doxorubicin induces apoptosis in normal and tumor cells via distinctly different mechanisms - Intermediacy of H2O2- and p53-dependent pathways. J Biol Chem. 2004;279:25535-25543.

3. Erttmann R, Erb N, Steinhoff A, Landbeck G. Pharmacokinetics of Doxorubicin in Man - Dose and Schedule Dependence. J Cancer Res Clin Oncol. 1988;114:509-513.

4. Maciel D, Figueira P, Xiao S, Hu D, Shi X, Rodrigues J*, et al.* Redox-responsive alginate nanogels with enhanced anticancer cytotoxicity. Biomacromolecules. 2013;14:3140-3146.

5. Lee DE, Koo H, Sun IC, Ryu JH, Kim K, Kwon IC. Multifunctional nanoparticles for multimodal imaging and theragnosis. Chem Soc Rev. 2012;41:2656-2672.

6. Pu KY, Liu B. Fluorescent Conjugated Polyelectrolytes for Bioimaging. Adv Funct Mater. 2011;21:3408-3423.

7. Waldo GS, Standish BM, Berendzen J, Terwilliger TC. Rapid protein-folding assay using green fluorescent protein. Nat Biotechnol. 1999;17:691-695.

8. Wang Y, Cao XY, Guo R, Shen MW, Zhang MG, Zhu MF*, et al.* Targeted delivery of doxorubicin into cancer cells using a folic acid-dendrimer conjugate. Polym Chem. 2011;2:1754-1760.

9. Shim MS, Kwon YJ. Stimuli-responsive polymers and nanomaterials for gene delivery and imaging applications. Adv Drug Deliver Rev. 2012;64:1046-1058.

10. Steinmetz NF, Ablack AL, Hickey JL, Ablack J, Manocha B, Mymryk JS*, et al.* Intravital imaging of human prostate cancer using viral nanoparticles targeted to gastrin-releasing Peptide receptors. Small. 2011;7:1664-1672.

11. Sokolova V, Epple M. Synthetic pathways to make nanoparticles fluorescent. Nanoscale. 2011;3:1957-1962.

12. Nagahama K, Mori Y, Ohya Y, Ouchi T. Biodegradable Nanogel Formation of Polylactide-Grafted Dextran Copolymer in Dilute Aqueous Solution and Enhancement of Its Stability by Stereocomplexation. Biomacromolecules. 2007;8:2135-2141.

13. Yallapu MM, Jaggi M, Chauhan SC. Design and engineering of nanogels for cancer treatment. Drug Discov Today. 2011;16:457-463.

14. Kopecek J. Hydrogel biomaterials: a smart future? Biomaterials. 2007;28:5185-5192.

15. Xiao C, Chen S, Zhang L, Zhou S, Wu W. One-pot synthesis of responsive catalytic Au@PVP hybrid nanogels. Chem Commun. 2012;48:11751-11753.

16. Kabanov AV, Vinogradov SV. Nanogels as Pharmaceutical Carriers: Finite Networks of Infinite Capabilities. Angew Chem Int Edit. 2009;48:5418-5429.

17. Park SY, Baik HJ, Oh YT, Oh KT, Youn YS, Lee ES. A Smart Polysaccharide/Drug Conjugate for Photodynamic Therapy. Angew Chem Int Edit. 2011;50:1644-1647.

18. Hasegawa U, Nomura SIM, Kaul SC, Hirano T, Akiyoshi K. Nanogel-quantum dot hybrid nanoparticles for live cell imaging. Biochem Bioph Res Co. 2005;331:917-921.

19. Ahmad Z, Pandey R, Sharma S, Khuller GK. Pharmacokinetic and pharmacodynamic behaviour of antitubercular drugs encapsulated in alginate nanoparticles at two doses. Int J Antimicrob Ag. 2006;27:409-416.

20. Li Y, Rodrigues J, Tomás H. Injectable and biodegradable hydrogels: gelation, biodegradation and biomedical applications. Chem Soc Rev. 2012;41:2193-2221.

21. Oh JK, Drumright R, Siegwart DJ, Matyjaszewski K. The development of microgels/nanogels for drug delivery applications. Prog Polym Sci. 2008;33:448-477.

22. Khdair A, Handa H, Mao GZ, Panyam J. Nanoparticle-mediated combination chemotherapy and photodynamic therapy overcomes tumor drug resistance *in vitro*. Eur J Pharm Biopharm. 2009;71:214-222.

23. Khdair A, Chen D, Patil Y, Ma L, Dou QP, Shekhar MP*, et al.* Nanoparticle-mediated combination chemotherapy and photodynamic therapy overcomes tumor drug resistance. J Control Release. 2010;141:137-144.

24. Li Y, Maciel D, Tomás H, Rodrigues J, Ma H, Shi XY. pH sensitive Laponite/alginate hybrid hydrogels: swelling behaviour and release mechanism. Soft Matter. 2011;7:6231-6238.

25. Oliveira JM, Salgado AJ, Sousa N, Mano JF, Reis RL. Dendrimers and derivatives as a potential therapeutic tool in regenerative medicine strategies-A review. Prog Polym Sci. 2010;35:1163-1194.

26. Svenson S, Chauhan AS. Dendrimers for enhanced drug solubilization. Nanomedicine. 2008;3:679-702.

27. Medina SH, El-Sayed MEH. Dendrimers as Carriers for Delivery of Chemotherapeutic Agents. Chem Rev. 2009;109:3141-3157.

28. Taghavi Pourianazar N, Mutlu P, Gunduz U. Bioapplications of poly(amidoamine) (PAMAM) dendrimers in nanomedicine. J Nanopart Res. 2014;16:2342.

29. Wang SH, Shi XY, Van Antwerp M, Cao ZY, Swanson SD, Bi XD*, et al.* Dendrimer-functionalized iron oxide nanoparticles for specific targeting and imaging of cancer cells. Adv Funct Mater. 2007;17:3043-3050.

30. Vinogradov SV. Polymeric nanogel formulations of nucleoside analogs. Expert Opin Drug Deliv. 2007;4:5-17.

31. Gonçalves M, Figueira P, Maciel D, Rodrigues J, Qu X, Liu C*, et al.* pH-sensitive Laponite®/doxorubicin/alginate nanohybrids with improved anticancer efficacy. Acta Biomater. 2014;10:300-307.

32. Bushman J, Vaughan A, Sheihet L, Zhang Z, Costache M, Kohn J. Functionalized nanospheres for targeted delivery of paclitaxel. J Control Release. 2013;171:315-321.

33. Champion JA, Walker A, Mitragotri S. Role of particle size in phagocytosis of polymeric microspheres. Pharm Res. 2008;25:1815-1821.

34. Poon Z, Lee JB, Morton SW, Hammond PT. Controlling in Vivo Stability and Biodistribution in Electrostatically Assembled Nanoparticles for Systemic Delivery. Nano Lett. 2011;11:2096-2103.

35. Lamelas C, Avaltroni F, Benedetti M, Wilkinson KJ, Slaveykova VI. Quantifying Pb and Cd Complexation by Alginates and the Role of Metal Binding on Macromolecular Aggregation. Biomacromolecules. 2005;6:2756-2764.

36. Jin GW, Koo H, Nam K, Kim H, Lee S, Park JS*, et al.* PAMAM dendrimer with a 1,2-diaminoethane surface facilitates endosomal escape for enhanced pDNA delivery. Polymer. 2011;52:339-346.

37. Guillemet F, Piculell L. Interactions in Aqueous Mixtures of Hydrophobically-Modified Polyelectrolyte and Oppositely Charged Surfactant - Mixed Micelle Formation and Associative Phase-Separation. J Phys Chem. 1995;99:9201-9209.

38. Chen SC, Wu YC, Mi FL, Lin YH, Yu LC, Sung HW. A novel pH-sensitive hydrogel composed of N,O-carboxymethyl chitosan and alginate cross-linked by genipin for protein drug delivery. J Control Release. 2004;96:285-300.

39. Swietach P, Hulikova A, Patiar S, Vaughan-Jones RD, Harris AL. Importance of Intracellular pH in Determining the Uptake and Efficacy of the Weakly Basic Chemotherapeutic Drug, Doxorubicin. PLoS One. 2012;7:e35949.

40. Beijnen JH, Vanderhouwen OAGJ, Underberg WJM. Aspects of the Degradation Kinetics of Doxorubicin in Aqueous-Solution. Int J Pharm. 1986;32:123-131.

41. Gonçalves M, Figueira P, Maciel D, Rodrigues J, Shi X, Tomás H*, et al.* Antitumor Efficacy of Doxorubicin-Loaded Laponite/Alginate Hybrid Hydrogels. Macromol Biosci. 2014;14:110-120.

42. Jain K, Kesharwani P, Gupta U, Jain NK. Dendrimer toxicity: Let's meet the challenge. Int J Pharm. 2010;394:122-142.

43. Nasti A, Zaki NM, de Leonardis P, Ungphaiboon S, Sansongsak P, Rimoli MG*, et al.* Chitosan/TPP and Chitosan/TPP-hyaluronic Acid Nanoparticles: Systematic Optimisation of the Preparative Process and Preliminary Biological Evaluation. Pharm Res. 2009;26:1918-1930.

44. Schutz CA, Juillerat-Jeanneret L, Kauper P, Wandrey C. Cell response to the exposure to chitosan-TPP//alginate nanogels. Biomacromolecules. 2011;12:4153-4161.

45. Wojtkowiak JW, Verduzco D, Schramm KJ, Gillies RJ. Drug Resistance and Cellular Adaptation to Tumor Acidic pH Microenvironment. Mol Pharmaceut. 2011;8:2032-2038.

46. Santos JL, Oliveira H, Pandita D, Rodrigues J, Pêgo AP, Granja PL*, et al.* Functionalization of poly(amidoamine) dendrimers with hydrophobic chains for improved gene delivery in mesenchymal stem cells. J Control Release. 2010;144:55-64.

47. Wang SG, Wu YL, Guo R, Huang YP, Wen SH, Shen MW*, et al.* Laponite Nanodisks as an Efficient Platform for Doxorubicin Delivery to Cancer Cells. Langmuir. 2013;29:5030-5036.

Final Conclusions

In summary, nanogels based on alginate can be an excellent platform for biomedical applications, namely for anticancer drug delivery. The results of the present work show that alginate, a natural polymer, can be used for the preparation of nanogels with exceptional properties in terms of biocompatibility and ability of loading drugs (such as doxorubicin). Furthermore, it is possible to produce alginate nanogels that respond to environmental stimuli, including pH variations, and redox conditions. Due to their stimuli-responsiveness, these nanocarriers can preferentially deliver the drugs in cell specific sites, making them extraordinary carriers for cancer or even other diseases.

In Chapter II, a simple procedure for the preparation of redox-sensitive nanogels was reported. The synthesized nanogels (AG/Cys) were obtained *via* a miniemulsion method using cystamine as a crosslinker. Dox was loaded into the AG/Cys nanogels through electrostatic interactions between the anionic AG and the cationic Dox. The results demonstrated that the AG/Cys nanogels were cytocompatible, presented a high drug encapsulation efficiency, displayed an *in vitro* accelerated release of Dox in conditions mimicking the intracellular reductive environment, which could rapidly be internalized by CAL-72 cells, resulting in higher Dox intracellular accumulation, and a notable cell death when compared with free Dox. These nanogels may be an excellent platform to overcome the problem of Dox resistance in anticancer treatments and possibly be used for the delivery of other cationic drugs in applications beyond cancer.

In Chapter III, an easy process was used to develop dual-crosslinked AG/G5 nanogels, using calcium ions as crosslinkers and PAMAM G5 as co-crosslinkers, through an emulsion method. The dual-crosslinked AG/G5 nanogels showed a good cytocompatibility and were able of encapsulating the anticancer drug Dox. They displayed an improved drug release behavior when compared to the classical AG nanogels (those that used only calcium ions as crosslinkers). The biological studies showed that AG/G5 nanogels loaded with doxorubicin kept the anticancer cytotoxicity levels of free Dox and were successfully taken up by CAL-72 cells. The nanogels labeled with a fluorescent marker were shown to be useful for visualizing the nanogels inside cells by fluorescence microscopy. Thus, these resulting nanogels may serve as a general platform for therapeutic delivery and/or cell imaging.

UNIVERSIDADE da MADEIRA

CQM CENTRO DE QUÍMICA DA MADEIRA

Molecular Materials®
RESEARCH GROUP
MADEIRA ISLAND - PORTUGAL

FCT Fundação para a Ciência e a Tecnologia
MINISTÉRIO DA EDUCAÇÃO E CIÊNCIA

GOVERNO DA REPÚBLICA PORTUGUESA

UNIÃO EUROPEIA

REGIÃO AUTÓNOMA DA MADEIRA